THE ASTROPHYSICAL JOURNAL, 500:411–427, 1998 June 1

ACCRETION DISKS AROUND YOUNG OBJECTS. I. THE DETAILED VERTICAL STRUCTURE

PAOLA D'ALESSIO,[1] JORGE CANTÓ,[1] NURIA CALVET,[2,3] AND SUSANA LIZANO[1]

Received 1997 June 10; accepted 1998 January 23

ABSTRACT

We discuss the properties of an accretion disk around a star with parameters typical of classical T Tauri stars (CTTSs) and with the average accretion rate for these disks. The disk is assumed steady and geometrically thin. The turbulent viscosity coefficient is expressed using the α prescription, and the main heating mechanisms considered are viscous dissipation and irradiation by the central star. The energy is transported by radiation, turbulent conduction, and convection. We find that irradiation from the central star is the main heating agent of the disk, except in the innermost regions, $R < 2$ AU. The irradiation increases the temperature of the outer disk relative to the purely viscous case. As a consequence, the outer disk ($R > 5$ AU) becomes less dense, optically thin, and almost vertically isothermal, with a temperature distribution $T \propto R^{-1/2}$. The decrease in surface density at the outer disk decreases the disk mass by a factor of 4 with respect to a purely viscous case. In addition, irradiation tends to make the outer disk regions stable against gravitational instabilities.

Subject headings: accretion, accretion disks — radiative transfer — stars: pre–main-sequence

1. INTRODUCTION

The coplanarity and circularity of planetary orbits in our solar system support the idea that it has been formed from a rotating "protoplanetary disk," where energy is dissipated and momentum redistributed before the time of planet formation. Circumstellar disks are naturally formed during the collapse of a cloud fragment with nonzero angular momentum (Cassen & Moosman 1981; Tereby, Shu, & Cassen 1984). Disks produce observational signatures in the spectral energy distributions (SEDs) of young stellar objects (YSOs) in the form of excesses of emission at UV, IR, and millimeter wavelengths.

During the early evolutive phase of a forming star, the disk-star system is still surrounded by an infalling envelope, which dominates the far-IR SED. At longer wavelengths the infalling envelope becomes optically thin, and the SED is dominated by emission from the disk (Kenyon, Calvet, & Hartmann 1993; Calvet et al. 1994; Hartmann, Calvet, & Boss 1996). Radiation from the infalling envelope is one of the most important heating mechanisms of the disk in this early phase and has to be included to understand the long wavelength SEDs of embedded stars (e.g., Butner et al. 1991; Butner, Natta, & Evans 1994; D'Alessio, Calvet, & Hartmann 1997, hereafter DCH97)

There can be a transition phase in which the star and the disk are surrounded by a tenuous dusty envelope that scatters stellar radiation onto the disk (Natta 1993), heating its outer regions. But finally, in a more evolved phase, it is expected that the material surrounding the disk-star system becomes negligible (e.g., Shu, Adams, & Lizano 1987).

Models for accretion disks (Lynden-Bell & Pringle 1974) or flattened disks reprocessing stellar radiation (Adams, Lada, & Shu 1987) predict steeper SEDs than those observed in classical T Tauri stars. Kenyon & Hartmann (1987, hereafter KH) have proposed that a disk in vertical hydrostatic equilibrium, with well-mixed gas and dust, is flared and intercepts more stellar radiation than a flat disk. This model predicts a SED more similar to the observed ones, but it is restricted to wavelengths $\lambda < 100$ μm because of their assumption that the disk is optically thick.

In this paper, we explore the evolved phase in which the disk-star system is surrounded by a negligible amount of dust, adopting the basic idea behind the KH model, i.e., gas and dust in the disk are well mixed and thermally coupled. The disk receives radiation directly from the central star, and it is also heated by viscous dissipation, cosmic rays, and radioactive decay. We calculate the detailed vertical structure of such a disk, taking into account several transport mechanisms: turbulent flux, radiation, and convection. The disk interior and atmosphere are not arbitrarily separated. The complete structure, from the midplane to the surface, is calculated with the same set of equations, written in a general way to treat both optically thick and thin regions. We then present a detailed study of one case, with parameters typical of classical T Tauri stars.

In a forthcoming paper (D'Alessio et al. 1998b, hereafter Paper II) we show results of the structure and physical properties for a wide range of parameters characterizing disks and central stars. Finally, motivated by the large amount of observational information compiled in recent years, we calculate (D'Alessio et al. 1998a, hereafter Paper III) how the observational signatures of disks depend on their physical properties. Comparing models to observations of classical T Tauri stars, we infer disk's physical properties.

The structure of the present paper is as follows: in § 2 we present the assumptions and general description of the model; in §§ 3 and 4 we give a detailed discussion of the heating of the disk and the energy transport; in §§ 5 and 6 the equations and boundary conditions are written; in § 7 a particular case is discussed, with parameters typical of classical T Tauri disks; in § 8 we compare the model to a nonirradiated accretion disk and discuss the effects of irradiation; in § 9 the effect of the irradiation from an accretion ring is calculated; and finally § 10 presents a summary of the results.

[1] Instituto de Astronomía, Universidad Nacional Autónoma de México, A.P. 70-264, 04510 México D.F., México; dalessio@astroscu.unam.mx, lizano@astrosmo.unam.mx.

[2] Harvard-Smithsonian Center for Astrophysics, 60 Garden Street, Cambridge, MA 02138; ncalvet@medea.harvard.edu.

[3] On leave from Centro de Investigaciones de Astronomia, Mérida, Venezuela.

2. GENERAL DESCRIPTION OF THE MODEL

We assume that the disks are in *steady state*; thus, all their properties are time independent. We also assume that the disk is *geometrically thin*, so the radial energy transport is neglected and the vertical and radial structures are treated as decoupled problems (Lynden-Bell & Pringle 1974; Pringle 1981). The disk is assumed to be in *vertical hydrostatic equilibrium*. Since there can be turbulent and convective motions in the vertical direction, the assumption of hydrostatic equilibrium refers to the mean bulk motion of the gas and dust in the disk. These assumptions are basic for the model and cannot be relaxed without changing the disk structure equations and the numerical method used to integrate them. Additional assumptions required to quantify the disk physical properties are that the mass accretion rate $\dot{M}$ is uniform through the disk and that the turbulent viscosity is described by the α *viscosity prescription*. Therefore, the viscosity effective coefficient is given by $v_t = \alpha c_s H$, where c_s is the local sound speed, H is the local scale height of the gas, and α is a free parameter, which is assumed constant through the disk with the only constraint that $\alpha \leq 1$ (Shakura & Sunyaev 1973). This prescription could be relaxed if $\dot{M}(R)$ and $v_t(R, z)$ are given.

We consider that the disk is heated by viscous dissipation, radioactive decay, cosmic rays, and stellar irradiation. The first two mechanisms generate and deposit energy at each height. Cosmic rays and stellar irradiation penetrate the disk from the upper surface and interact with the material below. We assume that the disk is a mixture of gas and dust and that both components are thermally coupled and described by a unique temperature. The gas is locally heated or cooled by viscous dissipation, ionization by energetic particles, collisions with dust, dust and gas radiation, convection, and turbulent conduction. The dust grains are heated or cooled by radiation from the star and from the disk itself and also by collisions with gas particles. A more general description of the disk structure is required to calculate the disk vertical structure equations assuming that gas and dust have different temperatures. However, we assume that the collisional and/or radiative heating between gas and dust are efficient enough at every point in the disk and use only one mean temperature to describe both components.

Because the disk is steady, the energy absorbed is emitted and transported outward. The energy is transported by (1) a *turbulent flux*, computed self-consistently with the viscosity coefficient used to describe the viscous energy dissipation; (2) *radiation*, through the first two moments of the transfer equation; and (3) *convection*, described by the mixing length theory, taking into account that the convective elements lose energy by radiation and turbulent flux.

Given a central star, the important quantities in describing a disk model are $\dot{M}$, which gives the total energy flux generated by viscous dissipation at each annulus in the disk, and α, which quantifies the fraction of viscous flux produced at each height. The disk structure also depends on the central star properties, i.e., its mass M_*, radius R_*, and effective temperature T_*. The mass M_* is related to the depth of the stellar gravitational potential, which is the last source of energy in the accretion process. The stellar luminosity, related to T_* and R_*, controls the amount of energy introduced in the disk by stellar irradiation.

The following sections give the physical and mathematical description of these processes. The resultant set of equations is solved with appropriate boundary conditions to get the temperature and density at each radius and height of the disk. The disk geometry is shown schematically in Figure 1.

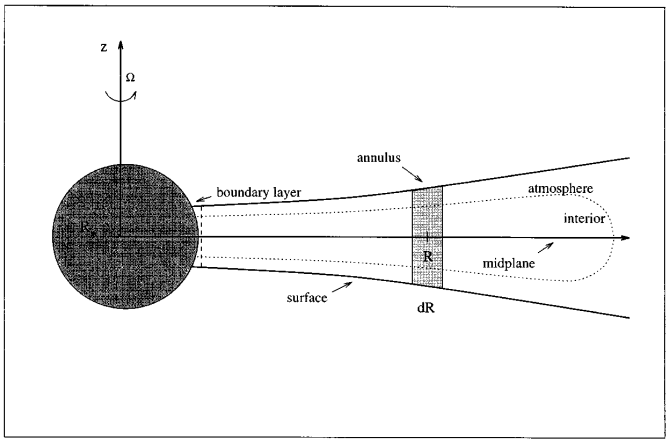

FIG. 1.—Geometry of the disk. This plot shows schematically what is called annulus, surface, atmosphere, interior, and midplane through the text. At a given distance R from the central star, the disk vertical structure refers to the disk physical properties in the z direction. The *atmosphere* refers to the optically thin part of the disk and the *interior* corresponds to the optically thick part; we indicate schematically that the outer regions become optically thin.

3. HEATING SOURCES

The disk heating sources are viscous dissipation, ionization by energetic particles, and stellar radiation. In this section we describe in detail each of these mechanisms and give the corresponding rates to be used in the calculation of the vertical structure.

3.1. *Viscous Dissipation*

The energy rate per unit volume locally generated by viscous stress is given by (Pringle 1981; Frank, King, & Raine 1992)

$$\Gamma_{\rm vis} = \tfrac{9}{4}\rho(z)v_t(z)\Omega(R)^2 = \tfrac{9}{4}\alpha P(z)\Omega(R)\,, \qquad (1)$$

where ρ is the mass density, P is the gas pressure, Ω is the Keplerian angular velocity, and v_t is the turbulent viscosity coefficient, given by $v_t = \alpha H c_s$.

The total energy per unit area produced by viscous dissipation in a given annulus at a distance R from the central star is thus,

$$F_{\rm vis}(z_\infty) = \int_0^{z_\infty} \Gamma_{\rm vis}\, dz = \frac{3GM_*\dot{M}}{8\pi} R^{-3}\left[1 - \left(\frac{R_*}{R}\right)^{1/2}\right], \qquad (2)$$

where z_∞ is the height of the disk and G is the gravitational constant.

3.2. *Ionization by Energetic Particles*

The main source of ionization by energetic particles is cosmic rays. However, Stepinski (1992) has shown that ionization due to energetic particles produced during the radioactive decay of ^{26}Al can be more important in those regions where cosmic rays cannot penetrate. We have thus considered both mechanisms, and the resulting heating rate

per unit volume is written as

$$\Gamma_{\rm ion}(\Sigma) = n_{\rm H_2}[\Delta Q_{\cos}\,\zeta_{\cos}\,e^{-\Sigma/\lambda} + \Delta Q_{\rm rad}\,\zeta_{\rm rad}(^{26}{\rm Al})]\ , \quad (3)$$

where $n_{\rm H_2}$ is the number density of hydrogen molecules and $\lambda = 96$ g cm^{-2} is the attenuation surface density scale of cosmic rays. The ionization rates due to cosmic rays and radioactive decay are $\zeta_{\cos} = 10^{-17}$ s^{-1} (Nakano & Umebayashi 1986) and $\zeta_{\rm rad}(^{26}{\rm Al}) = 5.2 \times 10^{-19}$ s^{-1} (Stepinski 1992), respectively, and Σ is the vertical column density from the disk surface to a height z. We have taken the energy liberated in heating in each cosmic ray ionization as $\Delta Q_{\cos} \approx 20$ eV and for radioactive decay ionization as $\Delta Q_{\rm rad} \approx 10$ eV Goldsmith & Langer (1978).

Integrating equation (3) in z, the total energy input per unit area due to ionization by energetic particles is given by

$$F_{\rm ion}(z_\infty) = \int_0^{z_\infty} \Gamma_{\rm ion}\,dz = \frac{1}{2m_{\rm H}}\left[\Delta Q_{\cos}\,\zeta_{\cos}\,\lambda(1 - e^{-\Sigma_\infty/2\lambda}) + \Delta Q_{\rm rad}\,\zeta_{\rm rad}\,\frac{\Sigma_\infty}{2}\right], \quad (4)$$

where $m_{\rm H}$ is the mass of the hydrogen atom and Σ_∞ is the total column density of the disk,

$$\Sigma_\infty = \int_{-z_\infty}^{z_\infty} \rho\,dz\ . \quad (5)$$

3.3. *Stellar Irradiation*

Following Calvet et al. (1991, hereafter CPMD), it is assumed that the stellar radiation intercepted by the disk consists of a parallel beam carrying a flux $F_{\rm irr}$ per unit area of the disk surface, incident at an angle $\theta_0 = \cos^{-1}\mu_0$ from the normal to the boundary of the disk atmosphere. A fraction of this energy is *scattered*, creating a diffuse field with wavelengths around the characteristic wavelength of the stellar radiation, given by the stellar effective temperature T_*. The remaining fraction of the incident radiation field is truly absorbed and remitted at wavelengths determined by the local temperature of the disk. As long as the characteristic temperature of the disk is lower than the effective temperature of the star, it can be assumed that no true emission of the disk occurs in the "stellar" frequency range and no scattering of the incident beam occurs in the "disk" frequency range.

The true absorption of radiation at the stellar frequency range is described through a Planck-type mean opacity, calculated evaluating the true absorption coefficient at the local temperature and pressure but using the Planck function evaluated at T_* as the weighting function. The resulting mean absorption coefficient is given by

$$\kappa_{\rm P}^*(T, P, T_*) = \frac{\pi}{\sigma_R\,T_*^4}\int_0^\infty \kappa_\nu(T, P)B_\nu(T_*)d\nu\ , \quad (6)$$

where κ_ν is the monochromatic true absorption coefficient, evaluated at the gas temperature T and gas pressure P, and σ_R is the Stefan-Boltzmann constant. The mean scattering coefficient $\sigma_{\rm P}^*(T, P, T_*)$ is calculated with the same kind of average given by equation (6), substituting κ_ν by σ_ν, the monochromatic scattering coefficient. The mean extinction coefficient is $\chi_{\rm P}^*(T, P, T_*) = \kappa_{\rm P}^* + \sigma_{\rm P}^*$. Since we assume that gas and dust are well mixed in the disk at every height, the absorption and scattering coefficients include the contribution of dust, unless it is sublimated in regions with a temperature higher than the sublimation temperature. If the dust has settled down in the midplane, the upper disk atmosphere would have a lower opacity to the stellar radiation than what we are assuming here.

The impinging stellar radiation field, which propagates in the direction defined by μ_0, reaches the height z with a flux given by

$$F_i(z) = -F_{\rm irr}\,e^{-\tau_s/\mu_0}\ , \quad (7)$$

where the optical depth τ_s is

$$\tau_s = \int_z^{z_\infty} \chi_{\rm P}^*\,\rho\,dz\ , \quad (8)$$

and the minus sign reflects the fact that this flux is going inward. The corresponding mean intensity is given by

$$J_i(z) = \frac{F_{\rm irr}}{4\pi\mu_0}\,e^{-\tau_s/\mu_0}\ . \quad (9)$$

The fraction of the incident radiation that is scattered is $s = \sigma_{\rm P}^*/\chi_{\rm P}^*$, and the fraction absorbed is $\kappa_{\rm P}^*/\chi_{\rm P}^* = 1 - s = a$. For simplicity, it is assumed that a and s are constant in the region where the stellar radiation is mainly absorbed (both fractions are evaluated at T and P such that $\tau_s = \frac{2}{3}$). This assumption will be checked a posteriori.

Following CPMD, the zero-order moment of the transfer equation for the diffuse radiation field can be written as

$$\frac{dF_s}{d\tau_s} = a4\pi J_s - s\,\frac{F_{\rm irr}}{\mu_0}\,e^{-\tau_s/\mu_0}\ , \quad (10)$$

where F_s and J_s are the flux and mean intensity of the diffuse stellar radiation field.

The first moment of the transfer equation, assuming the Eddington approximation (i.e., that the diffuse field is isotropic), is given by (Mihalas 1978)

$$\frac{dJ_s}{d\tau_s} = 3\,\frac{F_s}{4\pi}\ . \quad (11)$$

From equations (10) and (11), a second-order differential equation for J_s can be constructed. Given the boundary condition corresponding to an isotropic radiation field, i.e., $J_s = F_s/2\pi$, and assuming that s and a are independent of τ_s, the diffuse radiation field is described by

$$J_s = \frac{sF_{\rm irr}(2 + 3\mu_0)}{4\pi[1 + (2g/3)](1 - g^2\mu_0^2)}\,e^{-g\tau_s} - \frac{3\mu_0\,sF_{\rm irr}}{4\pi(1 - g^2\mu_0^2)}\,e^{-\tau_s/\mu_0}\ , \quad (12)$$

$$F_s = -\frac{gsF_{\rm irr}(2 + 3\mu_0)}{3[1 + (2g/3)](1 - g^2\mu_0^2)}\,e^{-g\tau_s} + \frac{sF_{\rm irr}}{(1 - g^2\mu_0^2)}\,e^{-\tau_s/\mu_0}\ , \quad (13)$$

where $g = (3a)^{1/2}$.

Finally, from equations (7) and (10), the disk heating rate per unit volume due to stellar radiation can be written as

$$\Gamma_{\rm irr} = \chi_{\rm P}^*\rho\left[4\pi aJ_s + (1 - s)\frac{F_{\rm irr}}{\mu_0}\,e^{-\tau_s/\mu_0}\right] = 4\pi\kappa_{\rm P}^*\,\rho(J_s + J_i)\,. \quad (14)$$

The irradiation flux $F_{\rm irr}$ is calculated as described by KH, with the disk height and shape calculated self-consistently, under the assumption of gas and dust well mixed and thermally coupled.

4. ENERGY TRANSPORT

In different regions of a given disk, different mechanisms could be responsible for the energy transport. With the aim of making a reliable model to cover a wide range of disk and stellar parameters, we have considered that the energy in the disk can be transported by radiation, convection, and turbulence. In the following we describe each of these mechanisms.

4.1. *Radiative Transport*

The disk's own radiation is characteristic of the disk local temperature, so it corresponds to lower frequencies with respect to those characteristic of the stellar radiation. The radiative transport at these frequencies is described through the first two moments of the transfer equation integrated in frequency, using the Eddington approximation to close the system (Mihalas 1978). Instead of mean opacities averaged taking as weighting functions the frequency-dependent mean intensity and flux (κ_J and χ_F, in Mihalas notation), the Planck and Rosseland mean opacities ($\kappa_{\rm P}$ and $\chi_{\rm R}$) have been used. These mean opacities are computed with a consistent set of monochromatic opacities (see CPMD and D'Alessio 1996, for details).

The first two moments of the transfer equation in a frequency range characteristic of the disk physical conditions can be written as

$$\frac{dF_d}{dz} = \Lambda_d - \Gamma_d = 4\pi\kappa_{\rm P}\,\rho\left(\frac{\sigma_R\,T^4}{\pi} - J_d\right), \tag{15}$$

$$\frac{dJ_d}{dz} = -3\chi_{\rm R}\,\rho\,\frac{F_d}{4\pi}\,. \tag{16}$$

In equation (15), Λ_d represents the radiative cooling rate per unit volume, and Γ_d, the heating rate per unit volume due to disk radiation (i.e., in the disk frequency range).

Finally, the energy per unit area per time transported by radiation is given by the direct stellar flux, the diffuse stellar flux, and the disk radiative flux, that is,

$$F_{\rm rad} = F_i + F_s + F_d\,. \tag{17}$$

4.2. *Turbulent Flux*

The turbulent elements responsible for the disk viscosity are also transporting energy in the vertical direction (Rüdiger, Elstner, & Tschäpe 1988). Here we have assumed that the turbulence in the disk is not generated by convection but by another mechanism (e.g., instabilities associated with magnetic fields, see Balbus & Hawley 1991, 1992; Hawley & Balbus 1991, 1992). So convection and turbulent fluxes are treated as different energy transport mechanisms, which can both be present in a given region of the disk.

An adiabatic turbulent element moving from a hot region to a colder one in a superadiabatic medium has, through its trajectory, an excess of energy with respect to the surrounding medium. It loses part of its energy doing work on the surrounding gas, and the rest of the energy is liberated when it finally dissolves, mixing with the medium. If the medium is subadiabatic, the rising adiabatic elements have less energy with respect to the ambient gas and cool the upper and cooler layers. Assuming there is no net vertical mean motion in the disk, there are the same number of elements rising and falling at each height, so the net energy interchanged between the turbulent elements and the medium along their path is zero. Only the excess or deficit of energy of the elements and the medium, just before dissolving, contributes to the net flux. If the turbulent elements are adiabatic, the turbulent energy flux is proportional to the entropy gradient, and, following Rüdiger et al. (1988), can be written as

$$F_{\rm turb} = -\rho T\,\frac{v_t}{P_r}\,\frac{dS}{dz} = \frac{\alpha(P + P_{\rm rad})}{\Omega P_r}\,g_z\left(\frac{\nabla}{\nabla_A} - 1\right), \tag{18}$$

where S is the specific entropy, ∇ is the gradient ($d\ln T/d\ln P$) of the medium, ∇_A is the adiabatic gradient (i.e., ∇ evaluated at constant entropy), and $P_{\rm rad}$ is the radiation pressure. The Prandtl number P_r is given by the ratio of the efficiency of momentum and energy transport by turbulent elements, i.e., $P_r = \nu_t/\chi_t$, where ν_t is the turbulent viscosity coefficient and χ_t is the turbulent conductivity coefficient. Finally, g_z is the z component of the stellar gravity, given by

$$g_z = \Omega^2\,\frac{z}{[1 + (z/R)^2]^{3/2}}\,. \tag{19}$$

4.3. *Convection*

The energy transport by convection is included through the mixing length theory (e.g., Cox & Giuli 1968), with a convective efficiency computed assuming that the eddies loose energy by turbulent flux and by radiation. The radiative losses are calculated estimating the optical depth of the elements (Mihalas 1978). The temperature gradient of the medium is calculated given the total flux of energy that has to be transported at each point. In order to calculate the energy transport by convection in both optically thin and thick convective regions of the disk and also to take into account that part of the total energy flux F is transported by turbulent conduction, instead of using the usual definition of radiative gradient ∇_R based on the diffusion approximation, we introduce the gradient $\nabla_{\rm RC}$. This is the gradient ($d\ln T/d\ln P$) of the medium when convection is absent and can be written as

$$\nabla_{\rm RC} \equiv \frac{F - F_{\rm rad}}{A_{\rm turb}} + \nabla_A\,, \tag{20}$$

where $A_{\rm turb} \equiv \alpha P g_z/\Omega P_r\,\nabla_A$ and we have used equation (18).

It is assumed the disk is unstable to convection in those regions where $\nabla_{\rm RC} > \nabla_A$. When this condition holds, the true gradient of the medium is given by

$$\nabla = (1 - \zeta)\nabla_{\rm RC} + \zeta\nabla_A\,, \tag{21}$$

where ζ is a convective efficiency and depends on the mixing length Λ, a free parameter of this convection theory (see D'Alessio 1996 for details). On the other hand, when $\nabla_{\rm RC} < \nabla_A$ the medium is stable against convection and energy is transported only by radiation and turbulent flux. In these regions $\nabla = \nabla_{\rm RC}$.

The quantity ∇ contains the information of the efficiency of the different energy transport mechanisms at each point in the disk. Given ∇, the differential equation for the kinetic

temperature can be written as

$$\frac{dT}{dz} = -\nabla \frac{T}{P} g_z \rho \,, \tag{22}$$

which describes the temperature structure required by the energy transport mechanisms and the assumption of steady state.

The adiabatic gradient ∇_A and other thermodynamical quantities used in this work have been calculated in the way described by Vardya (1965) and Mihalas (1967).

5. HYDROSTATIC EQUILIBRIUM

The disk is assumed in vertical hydrostatic equilibrium,

$$\frac{dP}{dz} = -\rho g_z - \frac{dP_{\rm rad}}{dz} \,, \tag{23}$$

where the radiation pressure $P_{\rm rad}$ is included because it could be important for disks with very high accretion rates or in low-density regions, like the upper atmosphere. The radiation pressure gradient is given by (see Mihalas 1978, p. 170)

$$\frac{dP_{\rm rad}}{dz} = \frac{\rho}{c} \int_0^\infty \chi_\nu F_\nu \, d\nu \,, \tag{24}$$

where χ_ν is the monochromatic opacity coefficient, F_ν is the monochromatic radiative flux, and c is the speed of light. Using the mean opacities and the radiative energy fluxes defined in §§ 3.3 and 4.1, the radiation pressure gradient can be approximated as

$$\frac{dP_{\rm rad}}{dz} \approx \frac{\rho}{c} \left[\chi_{\rm R} F_d + \chi_{\rm R}^*(F_s + F_i)\right]$$

$$= \frac{\rho}{c} \left[\chi_{\rm R}(F_{\rm rad} - F_s - F_i) + \chi_{\rm R}^*(F_s + F_i)\right] \,, \tag{25}$$

where $\chi_{\rm R}$ is the Rosseland mean opacity and $\chi_{\rm R}^*$ is a Rosseland type mean opacity calculated using the derivative of the Planck function evaluated at the stellar temperature as the weighting function.

6. EQUATIONS

From the previous discussion, the set of differential equations that describe the disk vertical structure is

$$\frac{dF_{\rm rad}}{dz} = \Lambda_d - \Gamma_d - \Gamma_{\rm irr} \,, \tag{26}$$

$$\frac{dJ_d}{dz} = -\frac{3}{4\pi} \chi_{\rm R}(P, T)\rho(F_{\rm rad} - F_s - F_i) \,, \tag{27}$$

$$\frac{dF}{dz} = \Gamma_{\rm vis} + \Gamma_{\rm ion} \,, \tag{28}$$

$$\frac{dT}{dz} = -\nabla(F_{\rm rad}, F, T, P) \frac{T}{P} g_z \rho \,, \tag{29}$$

$$\frac{dP_g}{dz} = -\rho g_z - \frac{dP_{\rm rad}}{dz} \,. \tag{30}$$

These equations are solved subject to the following boundary conditions.

At $z = z_\infty$

$$P_g = P_\infty \,, \tag{31}$$

where P_∞ is a fixed small and arbitrary value of the gas pressure at $z = z_\infty$ (we adopt $P_\infty = 10^{-9}$ din cm^{-2}). The total energy flux is

$$F = F_{\rm rad} = (F_{\rm vis} + F_{\rm ion})|_{z_\infty} \,. \tag{32}$$

The net flux produced by viscous dissipation at $z = z_\infty$ is $F_{\rm vis}(z_\infty)$, given by equation (2), and the net flux produced by energetic particles ionization at $z = z_\infty$ is $F_{\rm ion}(z_\infty)$ from equation (3). The turbulent and convective fluxes are zero, since by definition the eddies cannot get out from the disk surface. The stellar flux going into the disk at z_∞ is $F_{\rm irr}$. This flux is reprocessed by the disk and emerges from its surface at a frequency range characteristic of its photospheric temperature. From the steady state assumption, the incident stellar flux is equal to the emergent stellar reprocessed flux, both integrated in frequency. Thus, the net flux associated with the stellar irradiation is zero at z_∞ and it does not contribute to equation (32). All the energy flux emerging from the surface of the disk is transported by radiation, i.e., $F_{\rm rad}(z_\infty) = F(z_\infty)$. Finally,

$$J_d(z_\infty) = J_\infty = \frac{1}{2\pi} (F_{\rm vis} + F_{\rm ion} + F_{\rm irr} - F_s)|_{z_\infty} \,, \tag{33}$$

where the irradiation flux $F_{\rm irr}$ is the stellar flux intercepted by the disk surface. The mean intensity J_∞ at the disk frequency evaluated at the disk surface is calculated with the two stream approximation, subtracting the contribution of the diffuse radiation field to the total stellar flux because it is scattered in the stellar frequency range.

At $z = 0$

$$F = F_{\rm rad} = 0 \,, \tag{34}$$

i.e., at the disk midplane ($z = 0$) all the energy fluxes are zero because of the reflection symmetry.

This is a two boundary problem. The disk height z_∞ is an unknown boundary and has to be determined. Using a fourth-order Runge-Kutta, we solve a reduced set of equations corresponding to the diffusion approximation. This result is used as an initial guess for a relaxation method (Press et al. 1989) to integrate the full set of equations discussed above, taking z_∞ as an eigenvalue.

We assume in this work that the disk is not surrounded by any substantial external material (i.e., an envelope or a wind). With this assumption, we choose a small value for P_∞ such that any material above it has no effect on the vertical structure; with this value of P_∞, we find that the outer disk regions flare. However, we also find that for higher values of P_∞, there can be an outer region where the disk height has a maximum and then decreases with R, so that the slope of the disk surface becomes negative and the computed irradiation flux becomes zero. But to have higher values of P_∞, the disk should be in pressure equilibrium with some surrounding material. In this case, this material would be heated by the central star and could transport scattered and reprocessed stellar radiation to the deeper disk regions, which cannot "see" the star directly (Natta 1993; D'Alessio et al. 1997). If this quasi-isotropic heating was included, the outer disk regions would flare (D'Alessio 1996; D'Alessio et al. 1997).

7. RESULTS AND DISCUSSION

For a central star of given M_*, R_*, and T_*, a disk mass accretion rate $\dot{M}$ and a viscosity parameter α, the density

and temperature structure can be calculated by integrating equations (26) to (30). In this paper, we have chosen, as an example, a set of parameters that are typical of T Tauri stars in Taurus: $\dot{M} = 10^{-8}\ M_\odot\ \mathrm{yr}^{-1}$ (Valenti, Basri, & Johns 1993; Gullbring et al. 1998), $T_* = 4000$ K, $M_* = 0.5\ M_\odot$, and $R_* = 2\ R_\odot$ (Kenyon & Hartmann 1995). The assumed mass accretion rate is lower than the critical mass accretion rate that leads to thermal instability (see Kawazoe & Mineshige 1993; Bell & Lin 1994), justifying the steady state assumption of the present model. The last parameter is the viscosity coefficient α. The value of α is crucial for modeling of the vertical structure of accretion disks, but is not known observationally. For the model discussed in this paper we chose $\alpha = 0.01$. This value is consistent with angular momentum transport by turbulence initiated by the Balbus & Hawley (BH) magnetohydrodynamical instability (Balbus & Hawley 1991; Hawley & Balbus 1991; Balbus & Hawley 1992; Hawley & Balbus 1992; Gammie 1996). Also, as shown by D'Alessio (1996), T Tauri's observed SEDs at millimeter wavelengths can be fitted by irradiated disk models with different combinations of $\dot{M}$ and α. In particular, for $\dot{M} = 10^{-8}\ M_\odot\ \mathrm{yr}^{-1}$, the viscosity parameter which leads to a flux and slope around $\lambda = 2.7$ mm consistent with observations (Dutrey et al. 1996) is $\alpha = 0.01$. In two forthcoming papers, we will present (1) a grid of models to illustrate the effect of different parameters on the SEDs, and (2) a detailed comparison between models and observations, to determine the range of parameter space that yields the best fit to observed SEDs.

7.1. *Optical Depths*

Figure 2 shows the radial distribution of the Rosseland τ_R, the Planck τ_P, and the "stellar" $\tau_s/\mu_0(R, z_\infty)$ mean total optical depths, integrated from the surface to the midplane of the disk. In this model $\tau_R > 1$ for $R < 20$ AU. For larger radii the disk becomes optically thin, decreasing τ_R with radius. The disk is optically thick to the stellar radiation ($\tau_s/\mu_0 \gg 1$) although it can be optically thin to its own radiation ($\tau_R < 1$). This is a consequence of the shorter wavelength characterizing the stellar radiation (CPMD) and the fact that it penetrates in a slanted angle (CPMD; Malbet & Bertout 1991). The Rosseland optical depth decreases for small radii ($R < 0.1$ AU) because of the sublimation of dust, which is the main opacity source in the disk. At these radii the disk temperature becomes similar to the sublimation temperature, given approximately by $T_{sub} \approx 1800$–2000 K.

The difference between the Planck and Rosseland mean optical depths reflects the strong frequency dependence of the monochromatic opacities used to calculate the means. While τ_R controls the radiative transport in optically thick regions, τ_P controls the radiative cooling in optically thin regions. Because radiation is the most important mechanism in transporting energy inside the disk (see below) the characteristic temperatures are highly dependent on the radial distribution of τ_R and τ_P.

7.2. *Characteristic Temperatures*

Figure 3 shows the temperature at the disk midplane T_c and the photospheric temperature (where $\tau_R = \frac{2}{3}$) T_{phot}. For small radii ($R \lesssim 0.5$ AU in this model) flaring is not important and $T_{phot} \sim R^{-3/4}$ as in an irradiated flat disk. For larger radii, the disk curvature becomes important, increasing the amount of stellar flux intercepted and flattening the distribution of photospheric temperature, giving $T_{phot} \sim R^{-1/2}$. This result is consistent with the temperature distribution found by Miyake & Nakagwa (1995), for an optically thick flared disk, with gas and dust well mixed. We only show the photospheric temperature for regions where $\tau_R < \frac{2}{3}$; outside, it is not defined. A simple analytical approximation gives $T_{phot} \sim R^{-3/7}$ for the region where the disk flaring becomes important, assuming that the stellar radiation is deposited at a height $z_s \propto H$, where H is the gas

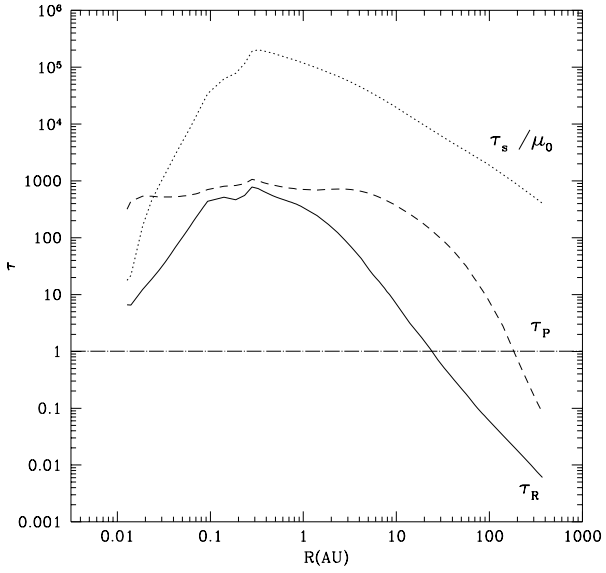

FIG. 2.—Radial distribution of different mean optical depths, integrated from the disk midplane to its surface. The disk parameters are $\dot{M} = 10^{-8}\ M_\odot\ \mathrm{yr}^{-1}$ and $\alpha = 0.01$, the central star parameters are $M_* = 0.5\ M_\odot$, $R_* = 2\ R_\odot$, and $T_* = 4000$ K. The vertical structure was calculated from $R = 0.0127$ to 373 AU. The plotted optical depths are Rosseland mean τ_R (*solid line*), Planck mean τ_P (*dashed line*), and the mean optical depth at the stellar frequency range $\tau_s/\mu_0(R, z_\infty)$ (*dotted line*). The horizontal line corresponds to $\tau = 1$.

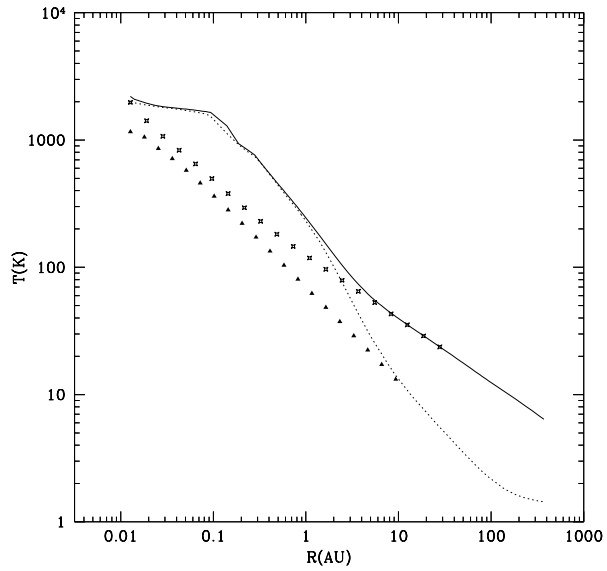

FIG. 3.—Radial distribution of the midplane T_c and photospheric T_{phot} temperatures for an irradiated and a nonirradiated disk model. The plotted temperatures are T_c for the irradiated disk (*solid line*), T_c for the nonirradiated disk (*dotted line*), T_{phot} for the irradiated disk (*stars*), and T_{phot} for the nonirradiated disk (*triangles*). The disk and stellar parameters are the same as Fig. 2.

pressure scale height (see Cantó, D'Alessio, & Lizano 1995). In this paper, the disk surface is assumed at constant pressure instead of proportional to the scale height, which results in a different radial dependence of the irradiation flux. We will show below that z_∞ is not proportional to H.

For $R \lesssim 2$ AU, viscous dissipation is the main energy source of the regions near the disk midplane. At larger radii, T_c becomes higher than the central temperature of a disk heated only by viscous dissipation, reflecting the importance of irradiation as a heating source. The contrast between T_c and $T_{\rm phot}$ depends on $\tau_{\rm R}$, since this optical depth controls the vertical temperature gradient required to transport the energy released at every height.

Figure 3 also shows that the central temperature distribution becomes flat around $T_c \sim 1800$–2000 K ($R \lesssim 0.1$ AU) where the Rosseland mean optical depth has a minimum (see Fig. 2). The dust is the dominant opacity source at temperatures lower than the sublimation temperature, which depends on the type of grain and the local density. In the regions where dust is destroyed the Rosseland mean opacity $\chi_{\rm R}$ decreases. At a given annulus, the optical depth increases toward the midplane (i.e., with a decreasing z), until a depth is reached where the dust is destroyed. From this height to the midplane the optical depth remains constant. In the region where dust is destroyed, the temperature is almost constant with height, being $T_c \sim T_{\rm sub}$ (see D'Alessio 1996). If the density were high enough to increase the optical depth toward the midplane (if there is a heating source at the disk midplane, e.g., viscous dissipation) then $T_c > T_{\rm sub}$. This is the case of disks with a lower α or a higher $\dot{M}$ than the model presented in this paper.

As can be seen in Figure 2, the Rosseland optical depth decreases with radius, so the gradient of temperature required to transport the energy produced in the disk also decreases with radius. The central temperature, for the optically thick annuli where the diffusion approximation holds, scales as $T_c \approx T_{\rm phot}\,(3\tau_{\rm R}/4)^{1/4}$. For $R \gtrsim 10$ AU, where $\tau_{\rm R} \lesssim 10$, the photospheric and the central temperatures become very similar, i.e., the disk *interior* is almost vertically isothermal. In this outer region, the temperature is given approximately by $T \approx 0.84(F_{\rm irr}/\sigma_R)^{1/4}$, as follows from equation (26), with $J = J_\infty = {\rm const}$, $T = {\rm const}$, assuming $\tau_{\rm P} \gg 1$, $F_{\rm irr} \gg F_{\rm vis}, F_{\rm ion}$, and neglecting the diffuse radiation field.

At a given annulus, the density decreases with height and thus the optically thick annuli have upper optically thin layers, i.e., a *disk atmosphere*. Figure 4 shows the vertical distribution of temperature of the reference model at different radii. For all the disk there is a *temperature inversion* produced by the stellar irradiation (see CPMD). This temperature inversion is due to two effects, previously explored by CPMD: (1) the stellar radiation penetrates the disk along a slanted direction so the optical depth along its trajectory is larger than the case of a penetration perpendicular to the disk surface (see also Malbet & Bertout 1991), and (2) the opacity of the disk material (dominated by dust) to the stellar radiation is larger than the disk opacity to its own radiation (due to the shorter frequencies of the former). Malbet & Bertout (1991) considered only the first effect, but the second effect is dominant as can be seen in Figure 4.

The main difference between CPMD's treatment and the model presented in this paper is that we calculate the disk optical depth self-consistently with the temperature and density vertical structure, while CPMD assume the disk interior is optically thick and that there is no viscous dissipation at the disk atmosphere, where energy is only transported. With the same set of equations, we calculate the optically thin atmosphere and the optically thick interior structures, without any assumption a priori about the optical depth of the different regions. Annuli situated at large distances from the star can be completely optically thin and the assumptions made by CPMD are not valid, while with the method described in this paper, the structure of the optically thin outer disk can be calculated. Thus, we have found that these regions have a temperature inversion, as the surface temperature is higher than the photospheric temperature. The annuli with low Rosseland mean optical depth are almost vertically isothermal between the midplane and the photosphere but have a large contrast in temperature between the photosphere and the disk surface.

Figure 4 also shows that the approximation found by CPMD, with a correction introduced by the use of the Planck mean opacity in equation (15), is a good description of the temperature in the disk atmosphere. The disk upper atmosphere, with a temperature higher than the photospheric temperature, is like the "superheated" layer proposed by Chiang & Goldreich (1997), where the stellar radiation penetrating the disk is deposited. The main difference with their treatment and this paper is that here the disk vertical structure is calculated in detail.

Figure 5 shows the surface temperature of the disk T_0, i.e., the temperature at z_∞. From $R \sim 0.5$ AU to 80 AU, T_0 is given approximately by $T_0 \sim R^{-0.56}$, and for larger radii we found $T_0 \sim R^{-2/5}$, which is consistent with the expected temperature of optically thin dust (with an absorption coefficient $\kappa_\lambda \propto 1/\lambda$) heated by stellar radiation (Spitzer 1978; see also Chiang & Goldreich 1997).

7.3. *Characteristic Heights*

There is not a unique definition of disk height. Figure 6 shows the disk photospheric height $z_{\rm phot}$, the scale height of the gas at the midplane temperature H, the height at which the stellar radiation is deposited z_s, and the height at which $P = P_\infty$ given by z_∞. There are clear differences between these heights that can be understood as follows.

The pressure scale height of the gas at the central temperature is given by

$$\frac{H}{R} = \frac{c_s(T_c)}{R\Omega(R)} = \left[\frac{kT_c R}{GM_* \mu(T_c, \rho_c) m_{\rm H}}\right]^{1/2}. \qquad (35)$$

If T_c/μ decreases with R slower than $1/R$, then the gas pressure scale height increases with R. The higher the central temperature, the larger the pressure scale height. Therefore stellar irradiation increases this scale height with respect to a purely viscous disk. For $R \gtrsim 6$ AU, $H \propto R^{5/4}$ as is expected from equation (35) when $T_c \propto R^{-0.5}$.

The photospheric height $z_{\rm phot}$ is defined as the height where $\tau_{\rm R} = \frac{2}{3}$, if the disk is optically thick. For $R \gtrsim 30$ AU the disk becomes optically thin and there is no photosphere. The ratio $z_{\rm phot}/H \approx 2.5$ is between 0.1 and 20 AU.

The absorption height z_s, given by the height at which $\tau_s/\mu_0 = 1$, is the height where the largest fraction of stellar radiation is absorbed. Figure 6 shows that z_s is larger than $z_{\rm phot}$ at every radius of the disk, reflecting the fact that the disk becomes optically thick to the stellar radiation above the depth at which it becomes optically thick to its own radiation. For $R \gtrsim 20$ AU the disk is optically thick to the stellar radiation and optically thin to its own radiation. At

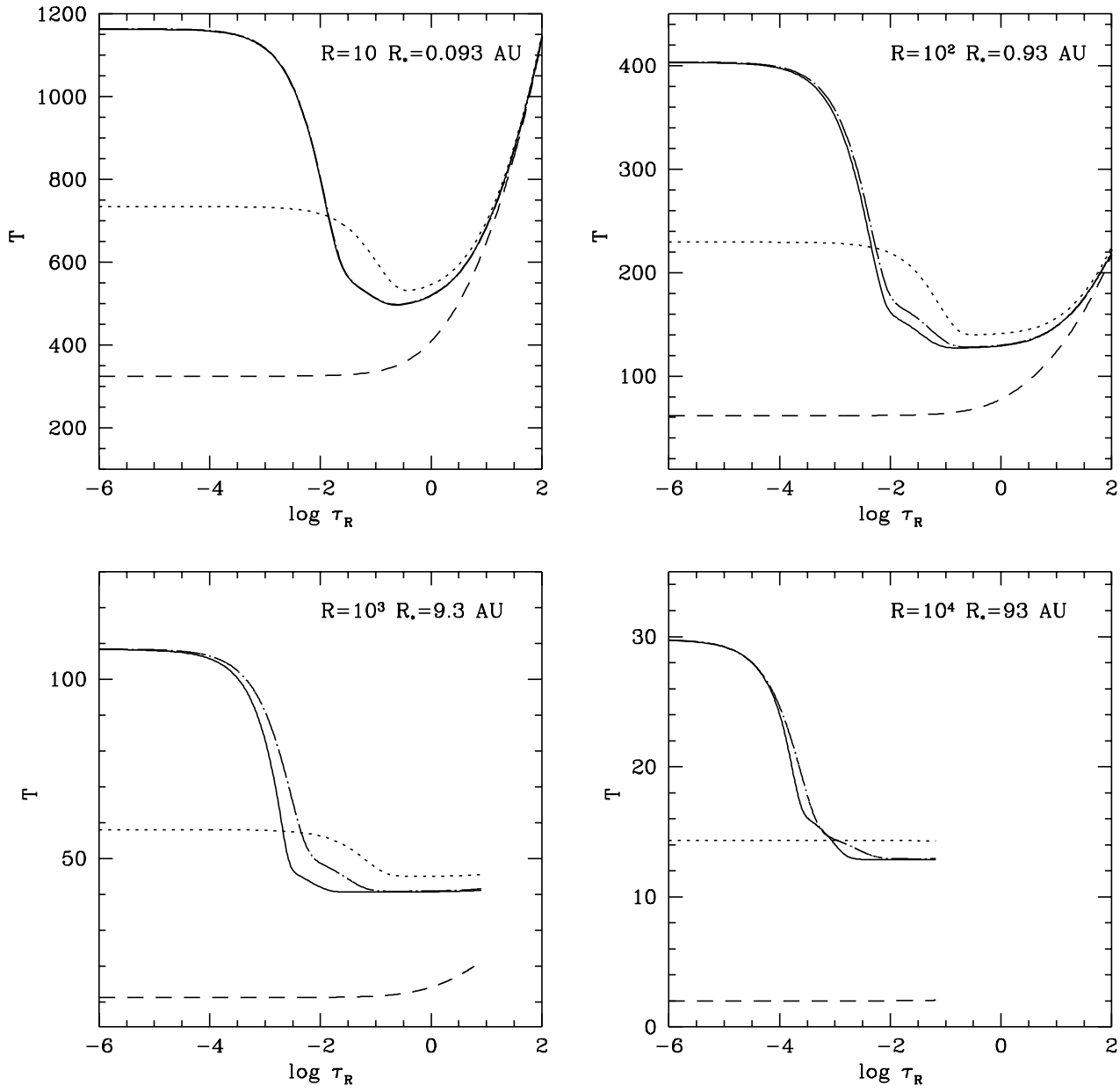

FIG. 4.—Vertical temperature distribution of an irradiated disk vs. logarithm of the Rosseland mean optical depth (integrated from the disk surface to z). The curves represent the temperature calculated in this paper (*solid line*), the temperature of a nonirradiated viscous disk (*dashed line*), the temperature given by CPMD (*dot-dashed line*), and the temperature calculated with the method of Malbet & Bertout (1991) (*dotted line*). Irradiation produces a temperature inversion toward the surface at all radii, the photosphere is at $\tau_R = \frac{2}{3}$. The disk and stellar parameters are the same as Fig. 2.

large distances from the star, z_s is close to the maximum height of the disk model z_∞.

From the vertical structure of this reference model, we find that z_s/H decreases from 4.5 to 2.5, when R changes from 10 to 300 AU. The ratio z_s/H is assumed constant in models where there is no vertical structure calculation (e.g., KH; Cantó et al. 1995; Chiang & Goldreich 1997) leading to $T_{\rm phot} \propto R^{-3/7}$ instead of $T_{\rm phot} \propto R^{-1/2}$.

The physical model considered in this paper is different from that described by Bell et al. (1997), where the disk is illuminated by a uniform radiation field with different temperatures (T = 10, 20, and 100 K). In that case, the relevant height is the *vertical* optical depth at the characteristic wavelength range of the incident radiation. Bell et al. (1997) find for the lowest radiation temperatures that the height decreases at large radii so that the outer disk regions cannot see the star. In the model studied in this paper, the radiation is coming from the central star (T_* = 4000 K), with a large incident angle with respect to the normal to the disk surface and also at shorter wavelengths. Both properties combine to produce a flared disk, with an absorption height increasing with radius. Therefore, when stellar irradiation is included in a self-consistent way, taking into account its characteristic wavelength and direction, the outer disk can be heated by the central star.

We can see that all the characteristic heights plotted in Figure 6 are less than R, supporting the thin disk approximation, used to decouple the vertical and radial structures.

7.4. *Surface Density*

Given the disk density as a function of R and z, the disk surface density radial distribution $\Sigma_\infty(R)$ is calculated using

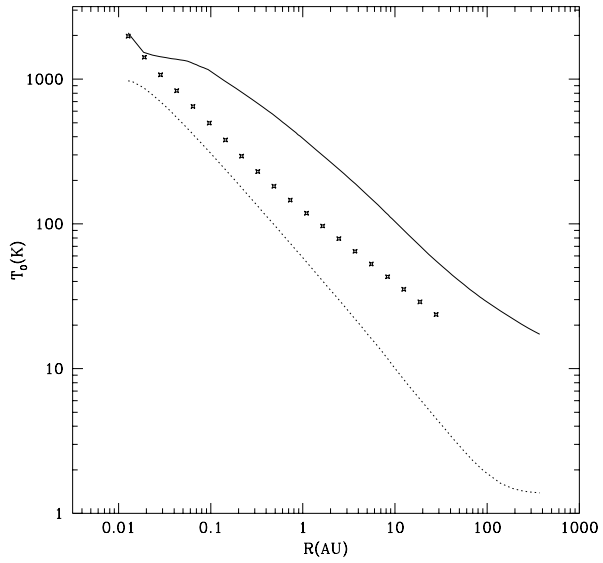

FIG. 5.—Temperature at the disk surface T_0 for an irradiated disk (*solid line*) and a nonirradiated disk (*dotted line*). The photospheric temperature $T_{\rm phot}$ of the irradiated disk is shown as a reference (*stars*). The disk and stellar parameters are the same as Fig. 2.

equation (5). Figure 7 shows $\Sigma_\infty(R)$ for an irradiated and a nonirradiated disk with the same $\dot{M}$, α, and central star. From the equation of conservation of angular momentum in a steady α disk, the surface density can be written as

$$\Sigma_\infty = \frac{\dot{M}}{3\pi\langle v_t\rangle}\left[1-\left(\frac{R_*}{R}\right)^{1/2}\right], \tag{36}$$

where $\langle v_t\rangle = \int_{-\infty}^{\infty} v_t(z, R)\rho(z, R)dz/\Sigma_\infty$ is a mean viscosity coefficient. Approximating $\langle v_t\rangle$ by the viscosity coefficient

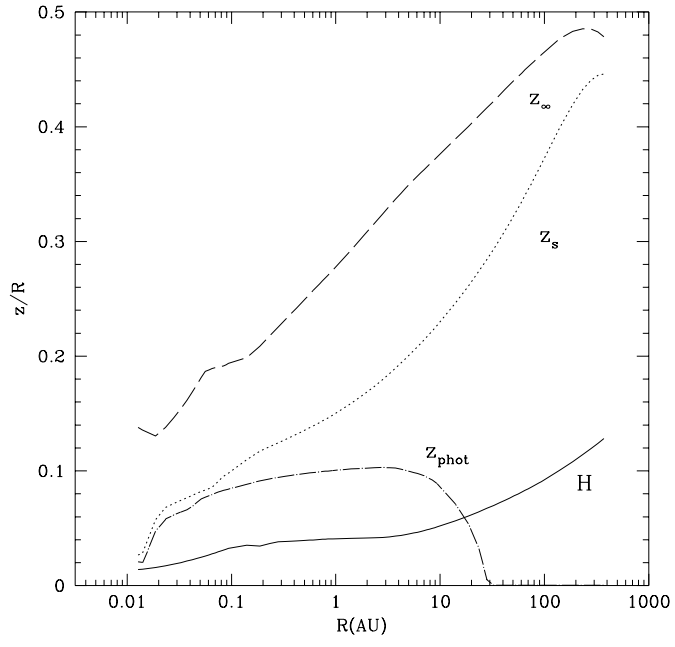

FIG. 6.—Radial distribution of different characteristic heights of an irradiated accretion disk. The plotted heights are the gas scale height H evaluated at the central temperature (*solid line*), the disk surface height z_∞ (*dashed line*), the height where a large fraction of stellar radiation is absorbed z_s (*dotted line*), and the photospheric height $z_{\rm phot}$ (*dot-dashed line*), all in units of the disk radius. The disk and stellar parameters are the same as Fig. 2.

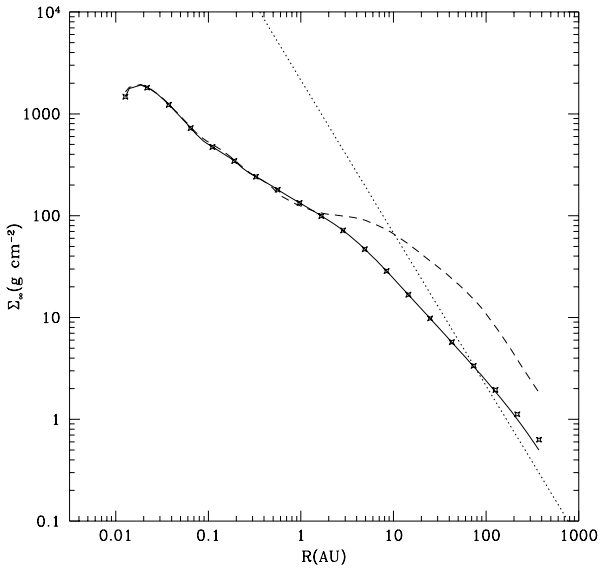

FIG. 7.—Radial distribution of surface density of an irradiated (*solid line*) and a nonirradiated (*dashed line*) disk model. For the irradiated disk, the approximation for Σ_∞ given by equation (37) is also plotted (*stars*). The nominal surface density $\Sigma \propto R^{-3/2}$, corresponding to the same total mass of the irradiated disk (assuming $R_d = 373$ AU), is also shown (*dotted line*; see text). The disk and stellar parameters are the same as Fig. 2.

evaluated at the disk midplane, the surface density can be written as

$$\Sigma_\infty \approx \frac{\dot{M}}{3\pi\alpha}\frac{\Omega\mu m_{\rm H}}{kT_c}\left[1-\left(\frac{R_*}{R}\right)^{1/2}\right]. \tag{37}$$

Figure 7 shows this expression for Σ_∞ compared to the surface density calculated numerically from $\rho(R, z)$. The approximation is a good description of the numerical result, which can be used as a check of the method used to integrate the vertical structure equations. From $R = 2$ to 100 AU, $\Sigma_\infty \sim R^{-1}$, as is expected from equation (37) when $T_c \sim R^{-0.5}$. Then, a steady α disk has a surface density distribution flatter than the nominal form $\Sigma_\infty = \Sigma_0 (R/R_*)^{-3/2}$, usually found in the literature (e.g., Beckwith et al. 1990; Dutrey et al. 1996; Miyake & Nakagwa 1995; Chiang & Goldreich 1997). Figure 7 also shows this power-law surface density for a disk with the same total mass (assuming $R_d = 100$ AU) as our reference model. The α irradiated disk has denser outer regions than the nominal model. This implies that the brightness of the outer disk is higher (for a fixed temperature distribution and opacity) at submillimeter and millimeter wavelengths, where the disk becomes optically thin. This result has implications on the physical properties of disks as inferred from observations at long wavelengths, which will be discussed in Paper III.

7.5. *Disk Mass*

The mass of a disk model is given by

$$M_d = \int_{R_i}^{R_d} \Sigma_\infty\, 2\pi R\, dR\,, \tag{38}$$

where R_i is the inner radius of the disk (which can be R_* if the disk extends inward to the surface of the star, or the radius of an inner hole R_h, when a magnetosphere is present; e.g., Gosh & Lamb 1979) and R_d is the outer radius of the disk. Because of the increase in surface area, M_d is determined by the mass of the outer regions, in spite of the

fact that the surface density decreases with R, as discussed above. From equation (37) we can see that except in the unlikely case of the central temperature increasing with R, the area of the annuli increases with R more rapidly than the decrease in Σ_∞. This result implies that the disk mass is not sensitive to the value of R_i (if $R_i \ll R_d$) and that the heating mechanisms, other than viscosity, affect strongly the mass of a disk model with fixed values of $\dot{M}$ and α.

Figure 8 shows the mass of the disk as a function of R_d. At $R_d = 100$ AU the disk mass is $M_d \approx 0.017\ M_\odot$, larger than the minimum mass of the solar nebula, $\sim 0.01\ M_\odot$, but smaller than the central star mass $M_* = 0.5\ M_\odot$. Therefore, it seems to be a good approximation to neglect the disk self-gravity with respect to the stellar gravity, as was assumed when the angular velocity of the disk was taken as the Keplerian angular velocity and, also, in the hydrostatic equilibrium equation.

Based on the result that the disk mass is determined by its outer regions, a rough estimation of M_d can be constructed assuming that the disk is vertically isothermal. Taking the midplane temperature as a power law, $T_c \approx T_1(R/R_1)^{-\gamma}$ for $R \geq R_1$ with $T_1 = T_c(R_1)$, and equations (37) and (38), the disk mass can be written as

$$M_d \approx M_{\rm inner}(R_1) + \frac{2\mu m_{\rm H}}{3kT_1} \times \sqrt{GM_* R_1}\,\frac{\dot{M}}{\alpha}\left(\gamma + \frac{1}{2}\right)^{-1}\left[\left(\frac{R_d}{R_1}\right)^{\gamma+1/2} - 1\right], \quad (39)$$

where $M_{\rm inner}(R_1)$ is the disk mass corresponding to regions with $R < R_1$, which we find is $M_{\rm inner}(R_1) \ll M_d(R_d)$ if $R_d \gg R_1$. For the reference model we find $R_1 \approx 456\ R_*$, $T_1 \approx 58$ K, and $\gamma \approx 0.5$. The mass $M_{\rm inner}(R_1) = 5 \times 10^{-4}\ M_\odot$, and $M_d \propto R_d$. Figure 8 shows the approximation described by equation (39) compared to the numerical result.

7.6. *Characteristic Timescales*

The lifetime of a disk with $\dot{M} = 10^{-8}\ M_\odot\ {\rm yr}^{-1}$ and $M_d = 0.017\ M_\odot$ is $M_d/\dot{M} \approx 1.7 \times 10^6$ yr. The characteristic time of the matter diffusion due to viscous torques $t_{\rm vis}$, is

$$t_{\rm vis} \approx \frac{R}{|u_R|} \approx \frac{R^2}{\langle v_t \rangle} = \frac{R^2\Omega}{\alpha c_s(T_c)}, \quad (40)$$

where u_R is the radial accretion speed.

The viscous time evaluated at R_d is an estimation of the lifetime of a disk that receives little mass from the surrounding cloud. Figure 9 shows that the reference model at 100 AU has $t_{\rm vis} \approx 2 \times 10^6$ yr, also consistent with the disk mean age $\sim 10^6$ yr, inferred from the position of T Tauri stars in the H-R diagram (Strom, Edwards, & Skrutski 1993).

From equation (40) we can see that the larger the central temperature, the shorter the lifetime of the disk, for a given value of α. Therefore, the stellar irradiation, which is the most important outer disk heating mechanism, cannot be neglected in a lifetime estimation of a given disk model.

7.7. *Energy Transport*

Figure 10 shows the fraction of the total energy flux transported by radiation, convection, and turbulence, as a function of height, at various distances from the central star. Also the position of the gas pressure scale height H is shown.

A flux with a positive sign is going in the $+z$ direction and with a negative sign is going in the $-z$ direction. In the convective regions (see the panel corresponding to $R = 0.093$ AU of Fig. 10) the turbulent flux is positive, thus it is transporting energy from inside to outside (from inner regions to upper regions).

Convection only transports an appreciable amount of energy near the midplane around $R = 10R_* \sim 0.01$ AU. In the radiative zones, the turbulent flux becomes negative, as can be seen from equation (18) when $\nabla < \nabla_A$. In these radiative or nonconvective regions, the turbulent flux transports energy from the upper layers, where temperature and pressure are low, to the inner layers, which are hotter and have a higher pressure. When a turbulent adiabatic eddy moves in a subadiabatic medium from a cold to a hot region, it will have a higher temperature with respect to the

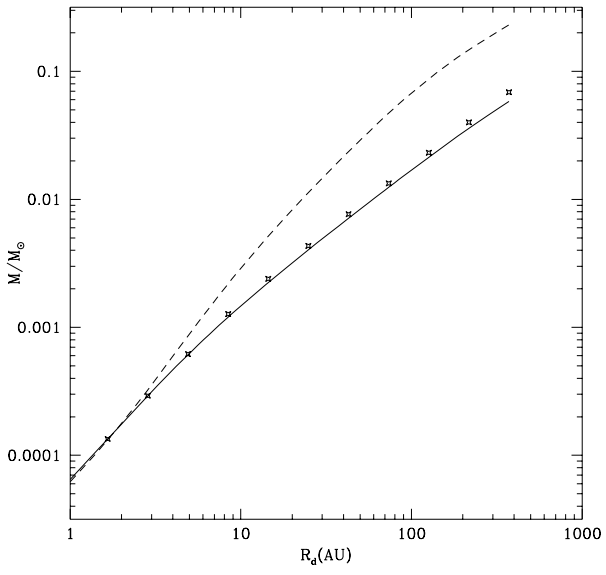

FIG. 8.—Radial distribution of total mass of an irradiated (*solid line*) and a nonirradiated (*dashed line*) disk model. The mass of the central star is $M_* = 0.5\ M_\odot$. For the irradiated disk, the approximation given by eq. (39) is also plotted (*stars*). The disk and stellar parameters are the same as Fig. 2.

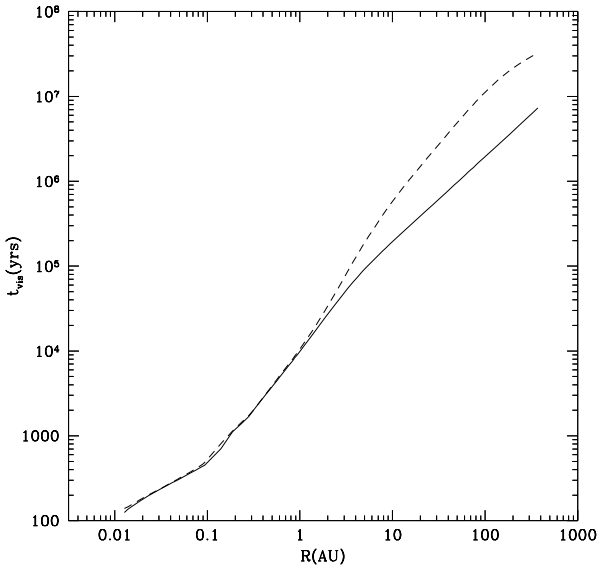

FIG. 9.—Radial distribution of the viscous time for an irradiated (*solid line*) and a nonirradiated (*dashed line*) disk as a function of radial distance to the central star. The mean disk age estimated (Strom et al. 1993) is $\sim 10^6$ yr. The disk and stellar parameters are the same as Fig. 2.

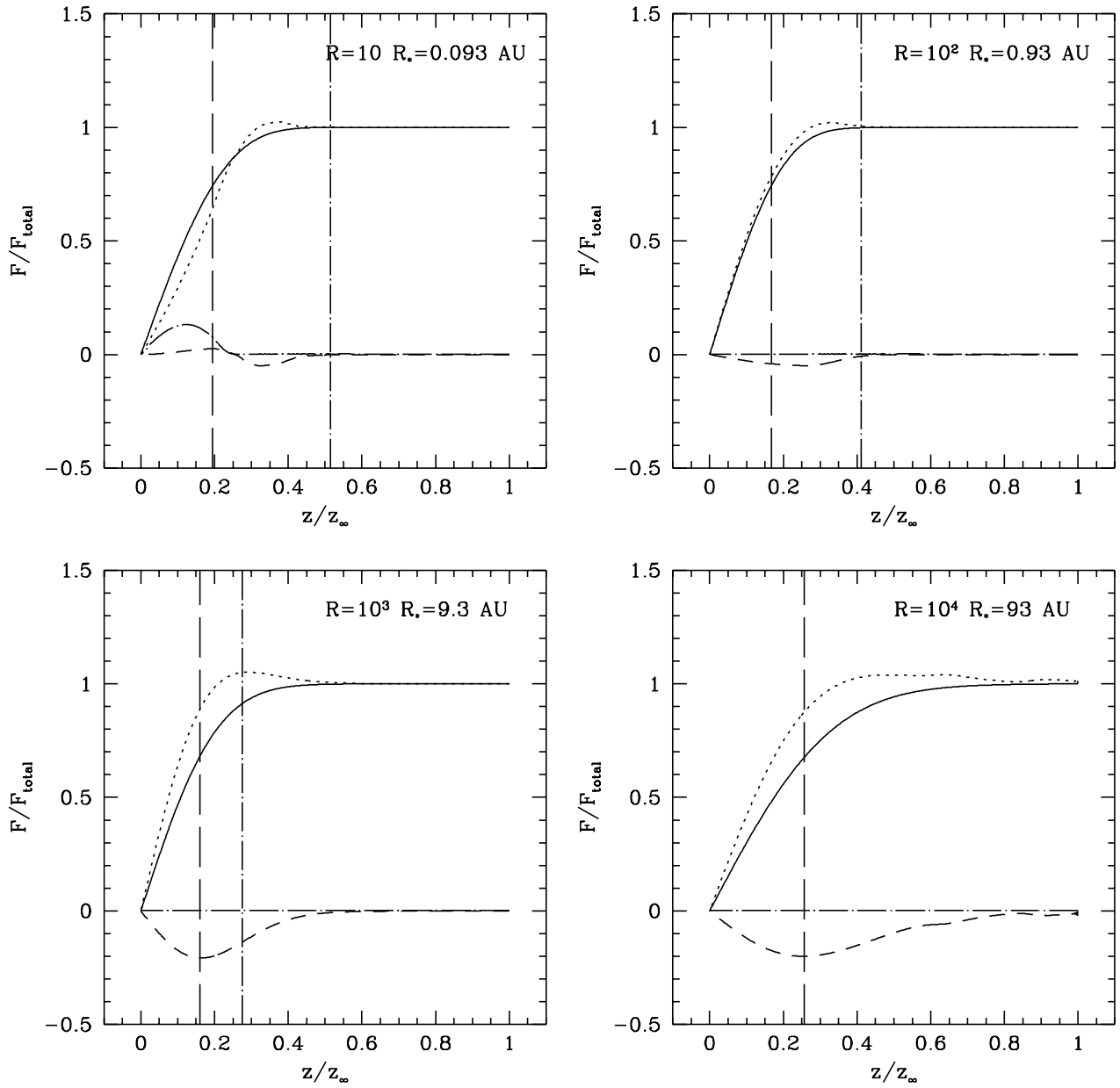

FIG. 10.—Vertical distribution of the fraction of total energy flux transported by different mechanisms for different annuli. The fluxes are total intrinsic flux (*solid line*), radiative flux (*dotted line*), turbulent flux (*dashed line*), and convective flux (*dot-dashed line*). The position of the gas scale height evaluated at the midplane temperature H is shown with a vertical dashed line, and the position of the photosphere is shown with a vertical dot-dashed line. Each panel shows at the upper corner the radius of the given annulus in units of stellar radius. The disk and stellar parameters are the same as Fig. 2.

surrounding medium. On the other hand, if this adiabatic eddy moves from a hot to a cold region, it will have a lower temperature with respect to the surrounding medium. The work made by the medium on the element or by it on the medium is responsible for this behavior. Therefore, the presence of the turbulent flux increases the radiative flux, as can be seen in Figure 10. At every annuli, we can see that radiation is the most important energy transport mechanism inside the disk, enhanced in the nonconvective regions because of the presence of the turbulent flux. Thus, radiation is controlling the disk temperature structure.

Note that less than 70% of the total flux is produced below the gas scale height. On the other hand, above the disk photosphere, the total flux is almost constant (see the panels corresponding to $R = 0.093, 0.93, 9.3$ AU in Fig. 10). So, it seems to be a good approximation to neglect the flux produced there by viscous dissipation and ionization due to energetic particles. Then, in the disk atmosphere, the energy is being only transported.

7.8. *Disk Gravitational Stability*

Another interesting physical property that can be calculated from a detailed disk model is the gravitational stability parameter introduced by Toomre (1964), which quantifies the fluid reaction against axisymmetric gravitational perturbations. The Toomre parameter can be written as

$$Q_T = \frac{c_s \Omega}{2\pi G \Sigma_\infty}, \tag{41}$$

such that, if $Q_T > 1$ the fluid is stable.

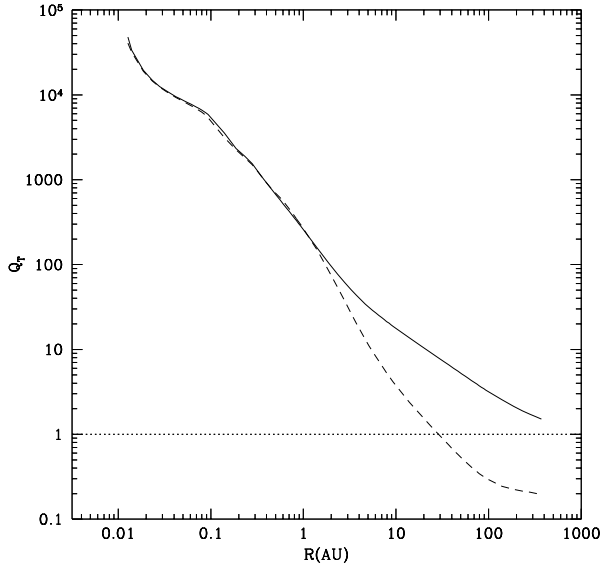

FIG. 11.—Radial distribution of Toomre's instability parameter Q_T for an irradiated (*solid line*) and a nonirradiated (*dashed line*) disk model. The value $Q_T = 1$ corresponds to the limit between stable and unstable regions (*dotted line*). The disk and stellar parameters are the same as Fig. 2.

Figure 11 shows Q_T as a function of R for the reference model; the disk is stable for the range of radii used to calculate the disk structure ($R \leq 337$ AU). It is interesting to note that if the irradiation flux is higher Q_T increases because of the increase in disk temperature and the decrease in surface density. Thus, irradiation tends to stabilize the disk against gravitational perturbations.

7.9. *Ionization Structure*

Given the vertical structure, it is interesting to evaluate where the ionization fraction (controlled by energetic particles and thermal ionization) is not enough to sustain the (BH) instability (Balbus & Hawley 1991). Gammie (1996) has called this region "the disk dead zone," where turbulent viscous dissipation cannot exist if the source of turbulence is the mentioned magnetic instability.

Following Gammie (1996), the ionization fraction that corresponds to a magnetic Reynolds number $\mathrm{Re}_M = V_A H/\eta = 1$, is given by

$$x_1 = 0.135 \times 10^{-13} \alpha^{-1/2} \left(\frac{R}{1\ \mathrm{AU}}\right)^{-3/2} \times \left(\frac{T}{500\ \mathrm{K}}\right)^{-1} \left(\frac{M_*}{M_\odot}\right)^{1/2}, \quad (42)$$

where V_A is the Alfvén speed, approximated as $V_A \approx \alpha^{1/2} c_s(T)$; η is the resistivity, given by $\eta = 6.5 \times 10^3 x^{-1}$ cm^2 s^{-1}; $x = n_e/n_H$ is the ionization fraction; and n_e is the electronic density.

On the other hand, from Stepinski (1992), the local ionization fraction due to energetic particles, considering recombination upon grain surfaces and ion reactions, can be written as

$$x_{ep} = 5.2 \times 10^{-18} r_{gr}^{-1} T^{1/2} \times \left\{ \sqrt{1 + 10^{-7} \frac{r_{gr}^2 [\zeta_{rad}(^{26}\mathrm{Al}) + \zeta_{cos} e^{-\Sigma/\lambda}]}{\rho^2 T}} - 1 \right\}, \quad (43)$$

where r_{gr} is the grain typical size (we adopt $r_{gr} = 0.1$ μm). The cosmic rays ionization rate decreases exponentially with the surface density, with a characteristic attenuation density given by ~ 100 g cm^{-2}. The thermal ionization fraction x_{th} is calculated assuming LTE and using the procedure described by Mihalas (1967). We approximate the ionization fraction in the disk as $x \approx \max(x_{th}, x_{ep})$.

Figure 12 shows a contour of $x/x_1 = 1$. In the region where $x < x_1$, the disk material is decoupled from the magnetic field, $\mathrm{Re}_M < 1$, and the BH instability cannot be the source of turbulence. This is the "dead zone," where there can be no viscous dissipation, and mass transport. In spite of the disk heating due to stellar irradiation, the thermal ionization is not enough in this region to make $\mathrm{Re}_M < 1$. If there is no other source of turbulence, the region between 0.2 and 4 AU cannot be treated with a constant $\dot{M}$ and α. Outside this region, the magnetic Reynolds number is $\mathrm{Re}_M > 1$ and the disk turbulence can be initiated by the BH instability.

As seen in Figure 12, the region where $x < x_1$ extends above the disk scale height, but it remains below the photosphere and the height where the stellar radiation is deposited. For $R \approx 2.5$ AU, the surface density in the dead zone is $\approx 90\%$ of the total surface density at this radius. At $R \sim 2$ AU the surface density drops below the attenuation scale for cosmic rays, ~ 100 g cm^{-2}, but the ionization fraction implied by equation (43) is smaller than the upper limit used by Gammie (1996), and x_{ep} remains less than x_1 between 2 and 4 AU.

7.10. *Spectral Energy Distribution*

For the reference model we have calculated the SED, assuming the disk is pole-on. The maximum and minimum radii adopted to calculate the SED are $R_d = 300$ AU and

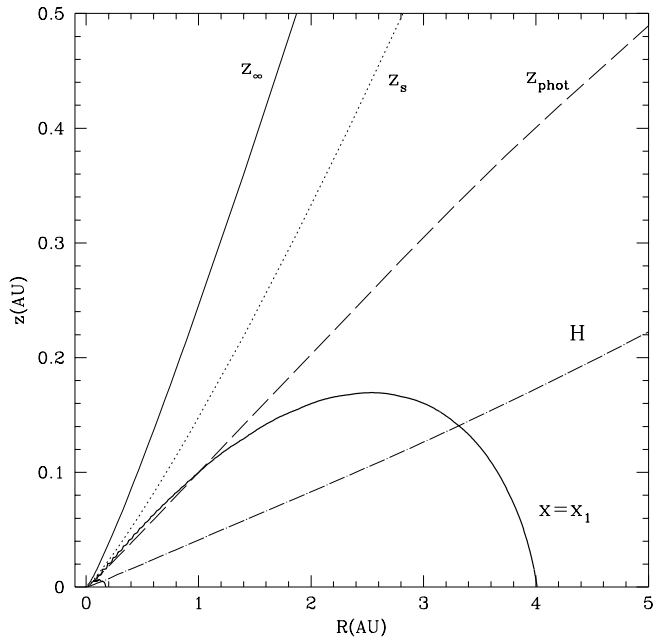

FIG. 12.—Contour of $x/x_1 = 1$, where x is the disk ionization fraction and x_1 is the ionization fraction corresponding to a magnetic Reynolds number $\mathrm{Re}_M = 1$. The region inside this contour, $0.2 < R < 4$ AU and $z < 0.17$, has $\mathrm{Re}_M < 1$. We also plot the disk height z_∞ (*solid line*), the height where a large fraction of the stellar radiation is absorbed z_s (*dotted line*), the photospheric height z_{phot} (*dashed line*), and the gas pressure scale height evaluated at the midplane H (*dot-dashed line*).

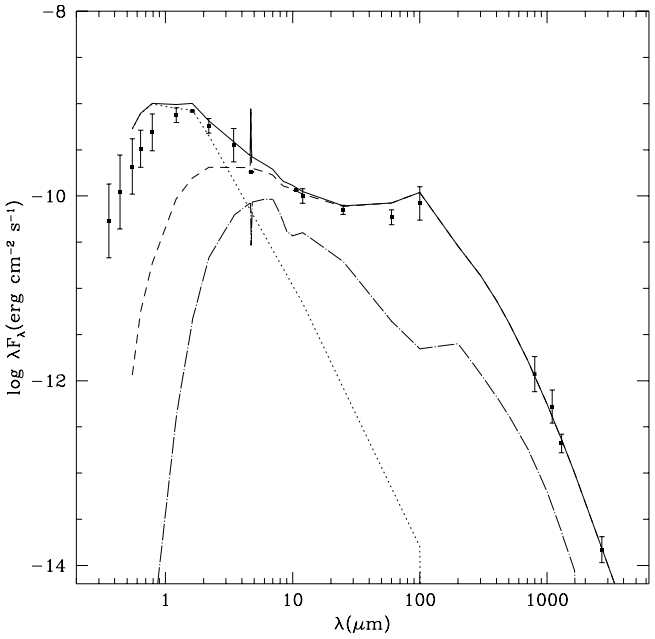

FIG. 13.—SED of the reference model pole-on, compared to AA Tau observed SED. The system's SED (star + disk) is shown with a solid line, the central star SED, taken from Bruzual & Charlot (1993), is plotted with a dotted line, and the disk SED is plotted with a dashed line. Also, the SED of a purely viscous disk with the same $\dot{M}$, α, and central star is shown with a dot-dashed line. The observational points (*squares*) were taken from Adams, Emerson, & Fuller (1990), Beckwith et al. (1990), Beckwith & Sargent (1991), Weaver & Jones (1992), Kenyon & Hartmann (1995), and Dutrey et al. (1996). The error bars are related to the variability of the object for $\lambda < 12$ μm and represent the reported errors for $\lambda \geq 12$ μm.

$R_{\rm hole} = 1\ R_*$, respectively. For the millimeter-wave dust opacity, we use a power law given by

$$\kappa_\nu = \kappa_0 \left(\frac{\lambda}{200\ \mu\text{m}} \right)^{-\beta}, \qquad (44)$$

where $\kappa_0 = 0.07$ cm^2 g^{-1} is obtained assuming that at wavelengths shorter than 200 μm the dust opacity is given by Draine & Lee (1984). The exponent β is taken as 1. This opacity is, at $\lambda = 1.3$ mm, a factor of 2.14 smaller than the opacity used by Beckwith et al. (1990).

Figure 13 shows the predicted SED compared to the SED of AA Tau, a typical classical T Tauri star, and the agreement is good for $\lambda > 2$ μm. We want to emphasize that this is not a best-fit model for AA Tau, it is only a typical model. In Paper III we will use observational restrictions as the mass accretion rate and central star properties inferred from optical observations to restrict the family of models for different particular objects. Nevertheless, the comparison between the SED of a typical model to the SED of a typical CTTS shows that the model predictions agree well with observations.

8. EFFECT OF STELLAR IRRADIATION ON THE DISK VERTICAL STRUCTURE

Disks can be irradiated by external sources, such as an infalling dense envelope (Butner et al. 1994; DCH97) or a tenuous dusty envelope, a remnant of the infalling envelope or associated with a disk or a stellar wind (Natta 1993), or the central star (Adams & Shu 1986; KH; CPMD; this paper). Different sources can be important in different evolutive phases of a disk, and in this paper we explore the case of a disk irradiated by the central star. A nonirradiated model is used to quantify the effects of stellar irradiation on the disk structure and physical properties, although it does not represent a realistic disk for the case treated here (with $\dot{M} = 10^{-8}\ M_\odot\ \text{yr}^{-1}$).

Irradiation is the main heating source of the disk. Also the heating due to ionization by energetic particles becomes larger than the viscous heating for $R > 200$ AU, but it is negligible with respect to the stellar irradiation. This behavior of the flux is reflected in the photospheric temperature distribution, plotted in Figure 3. For $R \lesssim 0.5$ AU, $T_{\rm phot}$ is similar to that of an irradiated "flat disk." For larger distances, $T_{\rm phot}$ becomes flatter than the temperature distribution of a viscous disk or a flat irradiated disk, $T_{\rm vis} \sim T_{\rm flat} \propto R^{-3/4}$. As shown in Figure 13, the irradiated disk has a larger emergent flux and a flatter SED at every wavelength than the nonirradiated disk. For $R \lesssim 2$ AU, T_c is the same for the irradiated and nonirradiated models because the viscous dissipation is the dominant heating source of the regions close to the disk midplane. At larger distances, the stellar radiation can penetrate the disk and it becomes the most important heating source at every height.

Figure 7 shows the surface density of the irradiated and nonirradiated disk model, with the same $\dot{M}$ and α. Stellar irradiation decreases the disk surface density for $R \gtrsim 1$ AU. As can be seen from equation (37), the change in disk temperature caused by the irradiation substantially increases the viscosity, and so, for a fixed mass accretion rate, the surface density drops correspondingly. The mass of the disk, determined by its surface density at large radii, also decreases with irradiation. As can be seen in Figure 8, the mass of a pure viscous disk with $\dot{M} = 10^{-8}\ M_\odot\ \text{yr}^{-1}$, $\alpha = 0.01$, and $R_d = 100$ AU is $M_d = 0.063\ M_\odot$, approximately a factor of 4 larger than an irradiated disk with the same $\dot{M}$ and α. From equation (39), a nonirradiated disk has $M_d \sim R_d^{7/4}$, assuming $\gamma \approx \frac{3}{4}$ in the outer regions, so its mass increases with the disk radius more rapidly than the mass of an irradiated disk $M_d \propto R_d$.

The increase in temperature produced by irradiation decreases the viscous time of the disk, as can be seen in Figure 9. The nonirradiated disk has $t_{\rm vis} \approx 10^7$ yr, an order of magnitude larger than the estimated mean lifetime of disks (Strom et al. 1993).

Another property for which the effect of irradiation is important is the Toomre instability parameter. Figure 11 shows that the nonirradiated disk becomes unstable for $R \gtrsim 28$ AU. The higher temperature and lower surface density of an irradiated disk, with respect to a pure viscous disk with the same α and $\dot{M}$, stabilizes the disk against gravitational perturbations for (at least) $R \lesssim 337$ AU.

9. EFFECT OF IRRADIATION FROM AN ACCRETION RING ON THE DISK STRUCTURE

The magnetospheric model has become widely accepted (e.g., Königl 1991; Calvet & Hartmann 1992; Shu et al. 1994). It is expected that the presence of a magnetosphere modifies the disk model discussed in this paper. Two important effects on the disk structure and emission are (1) to truncate the disk, such that the resulting inner hole decreases its near-IR emission, and (2) to heat the disk, changing its temperature and surface density distributions. The disk heating is produced by the interaction with the stellar magnetic field (Kenyon, Yi, & Hartmann 1996) and

also by radiation from an accretion shock at high stellar latitudes. For low-mass stars, this radiation is characterized by photons of much shorter wavelength than those of the stellar radiation or the local disk emission. Kenyon et al. (1996) conclude that the effect of this ring radiation is small, but they do not include the increased absorption efficiency due to the wavelength dependence of the opacity. In this section, we study the effect of the accretion ring radiation on the vertical structure of the reference model. The dependence of this additional heating source on disk and stellar parameters and its effect on physical (mass, stability, etc.) and observable (near-IR colors, long wavelength fluxes, etc.) properties of disks will be calculated in Papers II and III.

The calculation of the ring flux F_A intercepted by the disk and its mean incidence angle $\cos^{-1}\mu_A$ is described in the Appendix. The ring is located at an angle θ_0, measured from the z axis (see Fig. 14) and has an angular width $\Delta\theta_0$. We assume the ring has a temperature $T_A = 10{,}000$ K, inferred from the UV excess of T Tauri stars (e.g., Bertout, Basri, & Bouvier 1988). The ring angular width can be estimated as

$$\Delta\theta_0 = 0.057(\sin\theta_0)^{-1}\left(\frac{L_A}{L_\odot}\right)\left(\frac{T_A}{10^4\ \mathrm{K}}\right)^{-4}\left(\frac{R_*}{2\ R_\odot}\right)^{-2}\ \mathrm{rad}\ , \tag{45}$$

where L_A is the ring luminosity (for a ring seen pole-on by the observer). The ring luminosity can be related to the mass accretion rate (see Kenyon et al. 1996), writing:

$$L_A = 0.019\left(\frac{M_*}{0.5\ M_\odot}\right)\left(\frac{\dot{M}}{10^{-8}\ M_\odot\ \mathrm{yr}^{-1}}\right) \times \left(\frac{R_*}{2\ R_\odot}\right)^{-1}\left(2 - \frac{R_*}{R_{\mathrm{hole}}}\right)L_\odot\ . \tag{46}$$

The disk adopted as a reference model has $\Delta\theta_0 = 0.^\circ062/(\sin\theta_0)^{-1}\ (2 - R_*/R_{\mathrm{hole}})$. We have taken two values for $\theta_0 = 30°$, 60°, and an extreme value $(2 - R_*/R_{\mathrm{hole}}) = 2$, to explore the effect of the irradiation of a ring on the disk structure. The corresponding ring widths are $\Delta\theta_0 = 0.^\circ25$, for $\theta_0 = 30°$, and $\Delta\theta_0 = 0.^\circ14$, for $\theta_0 = 60°$. It is clear from equation (46) that the higher the $\dot{M}$, the larger the ring luminosity and the larger effect on the disk, at least on its upper layers or outer regions, where viscous dissipation can be less important.

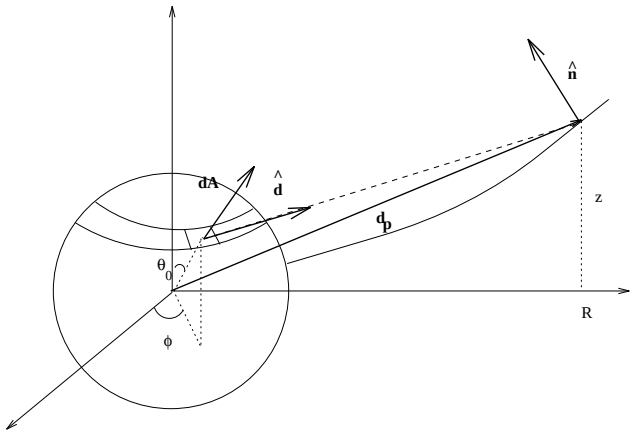

FIG. 14.—Geometry used to describe the irradiation of the disk due to a hot ring at the stellar surface.

We preserve the same set of equations and boundary conditions given in § 6, but now the irradiation flux F_{irr} is substituted by the stellar irradiation flux plus the ring flux, i.e.,

$$F_{\mathrm{irr}} = (1 - \Omega_A)F^*_{\mathrm{irr}} + F_A\ , \tag{47}$$

where Ω_A is the fraction of the solid angle subtended by the star, occupied by the ring (see the Appendix), and F^*_{irr} is the irradiation flux from the star (see KH).

The cosine of the angle of incidence is estimated as

$$\mu_0 = \left[\frac{(1/\mu_*)T_*^4(1 - \Omega_A) + (1/\mu_A)T_A^4\,\Omega_A}{T_*^4(1 - \Omega_A) + T_A^4\,\Omega_A}\right]^{-1}\ , \tag{48}$$

where $\cos^{-1}\mu_A$ is the averaged angle between the direction of the ring flux and the normal to the disk surface (see the Appendix), and $\cos^{-1}\mu_*$ is the mean angle between the stellar radiative flux and the normal to the disk surface. The Planck mean opacity, which describes the interaction between the disk material and the incident radiation field, is written as

$$\kappa_{\mathrm{P}}^{\mathrm{irr}} = \frac{\kappa_{\mathrm{P}}^*\,T_*^4(1 - \Omega_A) + \kappa_{\mathrm{P}}^A\,T_A^4\,\Omega_A}{T_*^4(1 - \Omega_A) + T_A^4\,\Omega_A}\ , \tag{49}$$

and the other mean opacities χ^{irr} and $\chi_{\mathrm{R}}^{\mathrm{irr}}$ are calculated with the same type of average. The mean "ring" opacities, κ_{P}^A, χ_{P}^A, and χ_{R}^A, are the mean opacities calculated using the Planck function evaluated at T_A as the weighting function (see eq. [6]).

At every radius, the irradiation flux from the star is larger than the irradiation flux from the ring. For $R > 0.1$ AU, the stellar flux is a factor of 10 larger than the ring flux. The ring irradiation increases the disk photospheric temperature less than 1%, in agreement with Kenyon et al. (1996). The temperature at the disk surface increases less than 6%.

10. SUMMARY AND CONCLUSIONS

In this paper we discuss a model of the vertical structure of steady and thin accretion disks, irradiated by their central stars, which includes transport of energy by radiation, convection, and turbulent flux. The radiative transport is treated without the diffusion approximation: The optically thin and thick regions of the disk are calculated with the same equations, without an a priori separation. We discuss the physical properties of a disk model with $\dot{M} = 10^{-8}\ M_\odot\ \mathrm{yr}^{-1}$ and $\alpha = 0.01$, around a low-mass star with $M_* = 0.5\ M_\odot$, $R_* = 2\ R_\odot$, and $T_* = 4000$ K, which represents a typical T Tauri disk. The effect of other input parameters on the structure and physical properties of disks will be reported in Paper II.

From this study, we conclude that the stellar irradiation is the main heating source of the outer regions ($R \gtrsim 1$–2 AU) in a typical T Tauri accretion disk, and has to be taken into account to calculate its physical properties, such as temperature, surface density, mass, height, lifetime, and gravitational stability. For instance, the photospheric and midplane temperature distributions of an irradiated disk are flatter than those of a nonirradiated viscous disk. The former case has a smaller surface density and, therefore, a smaller total mass than a nonirradiated viscous disk. Moreover, irradiation tends to stabilize the disk against gravitational perturbations, increasing the Toomre parameter above one. Therefore, if some of the disk properties are inferred from observations, they can be related to the disk

parameters $\dot{M}$ and α through a detailed model that must include the stellar irradiation.

Stellar irradiation produces a temperature inversion at the disk atmosphere, which, as shown by CPMD, has observational consequences. The sensitivity of the disk upper atmosphere temperature to the mean opacity suggests that it is important to make a detailed "model atmosphere" of the disk, solving the radiative transfer equation at different wavelengths and directions. Moreover, we have assumed that gas and dust are well mixed and thermally coupled. *Hubble Space Telescope* observations of HH 30 (Burrows et al. 1996) indicate that the dust scatters light from the central object and produces the observed image at scale heights $H/R \leq 0.1$, supporting the assumption that gas and dust are well mixed. Nevertheless, in order to evaluate both assumptions it seems necessary to calculate the disk structure considering gas and dust as separate ingredients with their particular dynamical and thermal behavior. This is a problem outside the scope of this paper, but we want to emphasize the importance of both assumptions. On the one hand, the gas is heated by viscous dissipation while dust is heated by stellar irradiation. If the collisional and radiative interaction between gas and dust is efficient enough, both can be characterized by the same temperature. On the other hand, if gas and dust are well mixed by turbulent motions, they have the same spatial distribution. In any case, given both assumptions, the height of the disk can be calculated self-consistently including the irradiation. A simple estimate of the difference in temperature between gas and dust, including only radiative and collisional heating of the gas particles by dust grains, shows that the assumption of a unique temperature is good below the disk photosphere. Nevertheless, the region where the stellar radiation is mainly absorbed has such low pressure that coupling is not very efficient. This can introduce an inconsistency in the atmospheric calculation discussed in the present paper, which has to be evaluated with a separate calculation of gas and dust temperatures. Also, as discussed by Chiang & Goldreich (1997), to calculate molecular line emission it is important to take into account the possibility that gas and dust have different temperatures in the upper atmosphere. In this sense, the present model corresponds to a first approximation to the atmospheric structure, which has to be evaluated with a more detailed treatment of the gas and dust thermal and dynamical behavior.

The accretion ring on the stellar surface can irradiate the disk. For the reference model this ring has a luminosity around 0.02–0.04 $L_\odot$ and a temperature around $T_A = 10{,}000$ K (from the UV excess of T Tauri stars). In this case, we found that the effect of this additional heating source on the disk structure and emission is negligible.

Our formalism can include any physical model that provides the viscosity ν as a function of *local* physical conditions in the disk. For the particular model discussed in this paper, we have used the α prescription, assuming a constant value of α throughout the disk, to evaluate ν. Given the vertical structure and following Gammie (1996), we have found the region where the ionization fraction (including thermal and energetic particles ionization) corresponds to a magnetic Reynolds number of $\mathrm{Re}_M < 1$, for a disk model with constant α. In the region where $\mathrm{Re}_M < 1$ the magnetic instability proposed by Balbus & Hawley (1991) cannot work. If the source of turbulence is this magnetic instability, then there cannot be viscous dissipation where $\mathrm{Re}_M < 1$, i.e., for $0.2 < R < 4$ AU, and this region will represent the dead zone of Gammie's model. In particular, Gammie proposes a "layered accretion" throughout this dead zone to alleviate the problem of the nonsteady behavior of accretion disks.

Finally, the predicted SED for the reference model is in agreement with the SED of AA Tau, for which preliminary results from Gullbring et al. (1998) are $\dot{M} = 3.8 \times 10^{-9}\ M_\odot$ yr^{-1}, $M_* = 0.53\ M_\odot$, $R_* = 1.74\ R_\odot$, and $T_* = 4048$ K. Both SEDs are shown in Figure 13. The wavelengths at which the SED is plotted are thought to sample the continuum spectrum and not to resolve lines and bands. Nevertheless, there are some apparent features in the irradiated disk SED, like the CO fundamental tone in emission around 4.3 μm and an IR band of water vapor around 100 μm. It is important to emphasize that these bands in emission are due to the atmospheric temperature inversion, and the assumption that gas and dust are thermally coupled. If this last assumption is not valid at the upper disk atmosphere, the details of the gas spectral features will change with respect to what is shown in Figure 13 (see Chiang & Goldreich 1997). Details of the disk SEDs, calculated for different inclination angles, will be discussed in a forthcoming paper.

We are grateful to Javier Ballesteros, Lee Hartmann, Alejandro Raga, and Salvador Curiel for helpful discussions. This work was supported in part by Instituto de Astronomía, UNAM, México, DGAPA-UNAM, ConaCyT, NAGW-2306, and NAG 5-4282.

APPENDIX

IRRADIATION OF THE DISK BY A HOT RING ON THE STELLAR SURFACE

In this appendix we describe the calculation of the flux intercepted by the disk, emergent from a hot annulus on the stellar surface. This annulus would correspond to the accretion shock between the material flowing through the stellar magnetosphere and the surface of the star. Figure 14 shows the geometry of this problem. The coordinate system and angles are defined in this figure.

A surface element of the hot annulus is given by

$$d\boldsymbol{A} = R_*^2\, d\Omega(\sin\theta\cos\phi\hat{\boldsymbol{x}} + \sin\theta\sin\phi\hat{\boldsymbol{y}} + \cos\theta\hat{\boldsymbol{z}})\,, \tag{A1}$$

where $d\Omega = \sin\theta\, d\theta\, d\phi$ is the solid angle of the surface element as seen from the center of the star. The same surface element, seen from a point P on the disk surface, has an apparent area dA_p, given by the projection of $d\boldsymbol{A}$ on $\hat{\boldsymbol{d}}$, where $\boldsymbol{d} = \boldsymbol{d}_p - \boldsymbol{r}$, $\boldsymbol{d}_p$ is

the vector describing the position of P, and $\boldsymbol{r}$ is the position vector of the annulus element, both given by

$$\boldsymbol{r} = R_*(\sin\theta\cos\phi\hat{\boldsymbol{x}} + \sin\theta\sin\phi\hat{\boldsymbol{y}} + \cos\theta\hat{\boldsymbol{z}}) , \tag{A2}$$

$$\boldsymbol{d}_p = R\hat{\boldsymbol{y}} + z_\infty\hat{\boldsymbol{z}} . \tag{A3}$$

Thus, the unit vector $\hat{\boldsymbol{d}}$ can be written as

$$\hat{\boldsymbol{d}} = \frac{\boldsymbol{d}_p - \boldsymbol{r}}{|\boldsymbol{d}_p - \boldsymbol{r}|} = \frac{-R_*\sin\theta\cos\phi\hat{\boldsymbol{x}} + (R - R_*\sin\theta\sin\phi)\hat{\boldsymbol{y}} + (z_\infty - R_*\cos\theta)\hat{\boldsymbol{z}}}{(R_*^2 + R^2 + z_\infty^2 - 2RR_*\sin\theta\sin\phi - 2z_\infty R_*\cos\theta)^{1/2}} \tag{A4}$$

The annulus element, as seen from point P, has a solid angle given by

$$d\Omega_p = \frac{dA_p}{d^2} = \frac{d\Omega R_*^2(R\sin\theta\sin\phi - R_* + z_\infty\cos\theta)}{(R_*^2 + R^2 + z_\infty^2 - 2RR_*\sin\theta\sin\phi - 2z_\infty R_*\cos\theta)^{3/2}} . \tag{A5}$$

The mean intensity of the annulus radiation field at point P is given by

$$J_\nu = \frac{1}{4\pi}\int I_\nu^A\, d\Omega_p . \tag{A6}$$

The flux intercepted by the disk is

$$F_A = \int_0^\infty\int I_\nu^A\,\mu\, d\Omega_p\, d\nu = \frac{\sigma_R T_A^4}{\pi}\int \mu\, d\Omega_p , \tag{A7}$$

where T_A is the ring effective temperature and μ is the cosine of the angle between the vector $\hat{\boldsymbol{d}}$, which characterizes the direction of incidence of the radiation, and the vector $\hat{\boldsymbol{n}}$, normal to the disk surface. The disk normal vector can be written as

$$\hat{\boldsymbol{n}} = \frac{-(dz_\infty/dR)\hat{\boldsymbol{y}} + \hat{\boldsymbol{z}}}{[1 + (dz_\infty/dR)^2]^{1/2}} . \tag{A8}$$

Thus,

$$\mu = -\hat{\boldsymbol{d}}\cdot\hat{\boldsymbol{n}} = \frac{(R - R_*\sin\theta\sin\phi)dz_\infty/dR - z_\infty + R_*\cos\theta}{[1 + (dz_\infty/dR)^2]^{1/2}(R_*^2 + R^2 + z_\infty^2 - 2RR_*\sin\theta\sin\phi - 2hR_*\cos\theta)^{1/2}} . \tag{A9}$$

Finally, substituting equation (A9) in equation (A7), the flux of the annulus intercepted by the disk can be calculated. The averaged value of the cosine of the angle between the incident radiation and the disk normal can be calculated as

$$\mu_A = -\frac{\int \hat{\boldsymbol{d}}\cdot\hat{\boldsymbol{n}}\, d\Omega_p}{\int d\Omega_p} . \tag{A10}$$

For simplicity, we assume that the annulus is at $\theta = \theta_0$ and it is thin enough to approximate the integrals over θ by the integrand evaluated at $\theta_0 \times \delta\theta_0$. For $R < (R_* - z_\infty\cos\theta_0)/\sin\theta_0$, the annulus is not *seen* by the disk. The integral over ϕ is symmetric with respect to $\phi = \pi/2$, so we make it from $\phi_{\min}$ to $\phi_{\max}$, and multiply the result by 2. The limits of this integration are given by

$$\phi_{\min} = \sin^{-1}\frac{R_* - z_\infty\cos\theta_0}{R\sin\theta_0} \tag{A11}$$

if $|R_* - z_\infty\cos\theta_0| \le |R\sin\theta_0|$, otherwise $\phi_{\min} = -\pi/2$ and $\phi_{\max} = \pi/2$.

REFERENCES

Adams, F. C., Emerson, J. P., & Fuller, G. A. 1990, ApJ, 357, 606
Adams, F. C., Lada, C. J., & Shu, F. H. 1987, ApJ, 312, 788
Adams, F. C., & Shu, F. H. 1986, ApJ, 308, 836
Balbus, S. A., & Hawley, J. F. 1991, ApJ, 376, 214
———. 1992, ApJ, 392, 662
Beckwith, S. V. W., & Sargent, A. I. 1991, ApJ, 381, 250
Beckwith, S. V. W., Sargent, A. I., Chini, R. S., & Guesten, R. 1990, AJ, 99, 1024
Bell, K. R., Cassen, P. M., Klahr, H. H., & Henning, Th. 1997, ApJ, 486, 372
Bell, K. R., & Lin, D. N. C. 1994, ApJ, 427, 987
Bertout, C., Basri, G., & Bouvier, J. 1988, ApJ, 330, 350
Bruzual, G., & Charlot, S. 1993, ApJ, 405, 538
Burrows, C. J., et al. 1996, ApJ, 473, 437
Butner, H. M., Evans, N. J., II, Lester, D. F., Levreault, R. M., & Strom, S. E. 1991, ApJ, 376, 636
Butner, H. M., Natta, A., & Evans, N. J., II. 1994, ApJ, 420, 326
Calvet, N., & Hartmann, L. 1992, ApJ, 386, 229
Calvet, N., Hartmann, L., Kenyon, S., & Whitney, B. 1994, ApJ, 434, 330
Calvet, N., Patiño, A., Magris, G., & D'Alessio, P. 1991, ApJ, 380, 617 (CPMD)
Cantó, J., D'Alessio, P., & Lizano, S. 1995, Rev. Mexicana Astron. Astrofis., 1, 217
Cassen, P., & Moosman, A. 1981, Icarus, 48, 353
Chiang, E. I., & Goldreich, P. 1997, ApJ, 490, 368
Cox, J. P., & Giuli, R. T. 1968, Principles of Stellar Structure (New York: Gordon & Breach)
D'Alessio, P. 1996, Ph.D. thesis, Universidad Nacional Autónoma de México, México
D'Alessio, P., Calvet, N., Cantó, J., & Lizano, S. 1998a, in preparation (Paper III)
D'Alessio, P., Calvet, N., & Hartmann, L. 1997, ApJ, 474, 397 (DCH97)
D'Alessio, P., Lizano, S., Cantó, J., & Calvet, N. 1998b, in preparation (Paper II)
Draine, B. T., & Lee, H. M. 1984, ApJ, 285, 89
Dutrey, A., Guilloteau, S., Duvert, G., Prato, L., Simon, M., Schuster, K., & Menard, F. 1996, A&A, 309, 493
Frank, J., King, A. R., & Raine, D. J. 1992, Accretion Power in Astrophysics (Cambridge: Cambridge Univ. Press), 72
Gammie, C. F. 1996, ApJ, 457, 355
Goldsmith, P. F., & Langer, W. D. 1978, ApJ, 222, 881
Gosh, P., & Lamb, F. K. 1979, ApJ, 232, 259

Gullbring, E., Hartmann, L., Briceño, C., & Calvet, N. 1998, ApJ, 492, 323
Hartmann, L., Calvet, N., & Boss, A. P. 1996, ApJ, 464, 387
Hawley, J. F., & Balbus, S. A. 1991, ApJ, 376, 223
———. 1992, ApJ, 400, 595
Kawazoe, E., & Mineshige, S. 1993, PASJ, 45, 715
Kenyon, S. J., Calvet, N., & Hartmann, L. 1993, ApJ, 414, 676
Kenyon, S. J., & Hartmann, L. 1987, ApJ, 323, 714 (KH)
———. 1995, ApJS, 101, 117
Kenyon, S. J., Yi, I., & Hartmann, L. 1996, ApJ, 462, 439
Königl, A. 1991, ApJ, 370, L39
Lynden-Bell, D., & Pringle, J. E. 1974, MNRAS, 168, 603
Malbet, F., & Bertout, C. 1991, ApJ, 383, 814
Mihalas, D. 1966, in Methods in Computational Physics, Vol. 7, ed. B. Alder, S. Fernbach & M. Rotenberg (New York: Academic), 1
———. 1978, Stellar Atmospheres (San Francisco: Freeman)
Miyake, K., & Nakagwa, Y. 1995, ApJ, 441, 361
Nakano, T., & Umebayashi, T. 1986, MNRAS, 218, 663
Natta, A. 1993, ApJ, 412, 761
Press, W. H., Flannery, B. P., Teukolsky, S. A., & Vetterling, W. T. 1989, Numerical Recipes (Cambridge: Cambridge Univ. Press)
Pringle, J. E. 1981, ARA&A, 19, 137
Rüdiger, G., Elstner, D., & Tschäpe, R. 1988, Acta Astron., 38, 299
Shakura, N. I., & Sunyaev, R. A. 1973, A&A, 24, 337
Shu, F. H., Adams, F. C., & Lizano, S. 1987, ARA&A, 25, 23
Shu, F. H., Najita, J., Ostriker, E., Wilkin, F., Ruden, S., & Lizano, S. 1994, ApJ, 429, 781
Spitzer, L. 1978, Physical Processes in the Interstellar Medium (New York: Wiley), 194
Stepinski, T. F. 1992, Icarus, 97, 130
Strom, S. E., Edwards, S., & Skrutski, M. F. 1993, Protostar and Planets III, ed. E. H. Levy & I. Lunine (Tucson: Univ. Arizona), 1031
Tereby, S., Shu, F. H., & Cassen, P. 1984, ApJ, 286, 529
Toomre, A. 1964, ApJ, 139, 1217
Valenti, J. A., Basri, G., & Johns, C. M. 1993, AJ, 106, 2024
Vardya, M. S. 1965, MNRAS, 129, 205
Weaver, W. M. B., & Jones, G. 1992, ApJS, 78, 239